virus pseudotypes into primary human hepatocytes by clathrin-dependent endocytosis. *J Gen Virol* **87**, 2583–2593.

Coller, K. E., Berger, K. L., Heaton, N. S., Cooper, J. D., Yoon, R. & Randall, G. (2009). RNA interference and single particle tracking analysis of hepatitis C virus endocytosis. *PLoS Pathog* **5**, e1000702.

Damke, H., Baba, T., van der Bliek, A. M. & Schmid, S. L. (1995). Clathrin-independent pinocytosis is induced in cells overexpressing a temperature-sensitive mutant of dynamin. *J Cell Biol* **131**, 69–80.

Damm, E. M., Pelkmans, L., Kartenbeck, J., Mezzacasa, A., Kurzchalia, T. & Helenius, A. (2005). Clathrin- and caveolin-1-independent endocytosis: entry of simian virus 40 into cells devoid of caveolae. *J Cell Biol* **168**, 477–488.

Evans, M. J., von Hahn, T., Tscherne, D. M., Syder, A. J., Panis, M., Wolk, B., Hatziioannou, T., McKeating, J. A., Bieniasz, P. D. & Rice, C. M. (2007). Claudin-1 is a hepatitis C virus co-receptor required for a late step in entry. *Nature* **446**, 801–805.

Grove, J. & Marsh, M. (2011). The cell biology of receptor-mediated virus entry. *J Cell Biol* **195**, 1071–1082.

Grove, J., Nielsen, S., Zhong, J., Bassendine, M. F., Drummer, H. E., Balfe, P. & McKeating, J. A. (2008). Identification of a residue in hepatitis C virus E2 glycoprotein that determines scavenger receptor BI and CD81 receptor dependency and sensitivity to neutralizing antibodies. *J Virol* **82**, 12020–12029.

Helle, F., Vieyres, G., Elkrief, L., Popescu, C.-I., Wychowski, C., Descamps, V., Castelain, S., Roingeard, P., Duverlie, G. & Dubuisson, J. (2010). Role of N-linked glycans in the functions of hepatitis C virus envelope proteins incorporated into infectious virions. *J Virol* **84**, 11905–11915.

Hoofnagle, J. H. (2002). Course and outcome of hepatitis C. *Hepatology* **36** (Suppl 1), S21–S29.

Kambara, H., Fukuhara, T., Shiokawa, M., Ono, C., Ohara, Y., Kamitani, W. & Matsuura, Y. (2012). Establishment of a novel permissive cell line for the propagation of hepatitis C virus by expression of microRNA miR122. *J Virol* **86**, 1382–1393.

Kataoka, C., Kaname, Y., Taguwa, S., Abe, T., Fukuhara, T., Tani, H., Moriishi, K. & Matsuura, Y. (2012). Baculovirus GP64-mediated entry into mammalian cells. *J Virol* **86**, 2610–2620.

Kato, N., Mori, K., Abe, K., Dansako, H., Kuroki, M., Ariumi, Y., Wakita, T. & Ikeda, M. (2009). Efficient replication systems for hepatitis C virus using a new human hepatoma cell line. *Virus Res* **146**, 41–50.

Liu, S., Yang, W., Shen, L., Turner, J. R., Coyne, C. B. & Wang, T. (2009). Tight junction proteins claudin-1 and occludin control hepatitis C virus entry and are downregulated during infection to prevent superinfection. *J Virol* **83**, 2011–2014.

Lupberger, J., Zeisel, M. B., Xiao, F., Thumann, C., Fofana, I., Zona, L., Davis, C., Mee, C. J., Turek, M. & other authors (2011). EGFR and EphA2 are host factors for hepatitis C virus entry and possible targets for antiviral therapy. *Nat Med* **17**, 589–595.

Marsh, M. & Helenius, A. (2006). Virus entry: open sesame. *Cell* **124**, 729–740.

Matlin, K. S., Reggio, H., Helenius, A. & Simons, K. (1981). Infectious entry pathway of influenza virus in a canine kidney cell line. *J Cell Biol* **91**, 601–613.

McKeating, J. A., Zhang, L. Q., Logvinoff, C., Flint, M., Zhang, J., Yu, J., Butera, D., Ho, D. D., Dustin, L. B., Rice, C. M. & Balfe, P. (2004). Diverse hepatitis C virus glycoproteins mediate viral infection in a CD81-dependent manner. *Journal of virology* **78**, 8496–8505.

Meertens, L., Bertaux, C. & Dragic, T. (2006). Hepatitis C virus entry requires a critical postinternalization step and delivery to early endosomes via clathrin-coated vesicles. *J Virol* **80**, 11571–11578.

Mercer, J., Schelhaas, M. & Helenius, A. (2010). Virus entry by endocytosis. *Annu Rev Biochem* **79**, 803–833.

Miaczynska, M. & Stenmark, H. (2008). Mechanisms and functions of endocytosis. *J Cell Biol* **180**, 7–11.

Mosso, C., Galván-Mendoza, I. J., Ludert, J. E. & del Angel, R. M. (2008). Endocytic pathway followed by dengue virus to infect the mosquito cell line C6/36 HT. *Virology* **378**, 193–199.

Norkin, L. C., Anderson, H. A., Wolfrom, S. A. & Oppenheim, A. (2002). Caveolar endocytosis of simian virus 40 is followed by brefeldin A-sensitive transport to the endoplasmic reticulum, where the virus disassembles. *J Virol* **76**, 5156–5166.

Pelkmans, L., Kartenbeck, J. & Helenius, A. (2001). Caveolar endocytosis of simian virus 40 reveals a new two-step vesicular-transport pathway to the ER. *Nat Cell Biol* **3**, 473–483.

Pileri, P., Uematsu, Y., Campagnoli, S., Galli, G., Falugi, F., Petracca, R., Weiner, A. J., Houghton, M., Rosa, D., Grandi, G. & Abrignani, S. (1998). Binding of hepatitis C virus to CD81. *Science* **282**, 938–941.

Ploss, A., Evans, M. J., Gaysinskaya, V. A., Panis, M., You, H., de Jong, Y. P. & Rice, C. M. (2009). Human occludin is a hepatitis C virus entry factor required for infection of mouse cells. *Nature* **457**, 882–886.

Sainz, B., Jr, Barretto, N., Martin, D. N., Hiraga, N., Imamura, M., Hussain, S., Marsh, K. A., Yu, X., Chayama, K. & other authors (2012). Identification of the Niemann–Pick C1-like 1 cholesterol absorption receptor as a new hepatitis C virus entry factor. *Nat Med* **18**, 281–285.

Scarselli, E., Ansuini, H., Cerino, R., Roccasecca, R. M., Acali, S., Filocamo, G., Traboni, C., Nicosia, A., Cortese, R. & Vitelli, A. (2002). The human scavenger receptor class B type I is a novel candidate receptor for the hepatitis C virus. *Embo J* **21**, 5017–5025.

Sieczkarski, S. B. & Whittaker, G. R. (2002a). Dissecting virus entry via endocytosis. *J Gen Virol* **83**, 1535–1545.

Sieczkarski, S. B. & Whittaker, G. R. (2002b). Influenza virus can enter and infect cells in the absence of clathrin-mediated endocytosis. *J Virol* **76**, 10455–10464.

Sumpter, R., Jr, Loo, Y.-M., Foy, E., Li, K., Yoneyama, M., Fujita, T., Lemon, S. M. & Gale, M., Jr (2005). Regulating intracellular antiviral defense and permissiveness to hepatitis C virus RNA replication through a cellular RNA helicase, RIG-I. *J Virol* **79**, 2689–2699.

Suzuki, T., Ishii, K., Aizaki, H. & Wakita, T. (2007). Hepatitis C viral life cycle. *Adv Drug Deliv Rev* **59**, 1200–1212.

Suzuki, R., Saito, K., Kato, T., Shirakura, M., Akazawa, D., Ishii, K., Aizaki, H., Kanegae, Y., Matsuura, Y. & other authors (2012). Trans-complemented hepatitis C virus particles as a versatile tool for study of virus assembly and infection. *Virology* **432**, 29–38.

Suzuki, R., Matsuda, M., Watashi, K., Aizaki, H., Matsuura, Y., Wakita, T. & Suzuki, T. (2013). Signal peptidase complex subunit 1 participates in the assembly of hepatitis C virus through an interaction with E2 and NS2. *PLoS Pathog* **9**, e1003589.

Trotard, M., Lepère-Douard, C., Régeard, M., Piquet-Pellorce, C., Lavillette, D., Cosset, F. L., Gripon, P. & Le Seyec, J. (2009). Kinases required in hepatitis C virus entry and replication highlighted by small interference RNA screening. *FASEB J* **23**, 3780–3789.

van der Schaar, H. M., Rust, M. J., Chen, C., van der Ende-Metselaar, H., Wilschut, J., Zhuang, X. & Smit, J. M. (2008). Dissecting the cell entry pathway of dengue virus by single-particle tracking in living cells. *PLoS Pathog* **4**, e1000244.

Vieyres, G., Thomas, X., Descamps, V., Duverlie, G., Patel, A. H. & Dubuisson, J. (2010). Characterization of the envelope glycoproteins associated with infectious hepatitis C virus. *J Virol* **84**, 10159–10168.

Zhong, J., Gastaminza, P., Cheng, G., Kapadia, S., Kato, T., Burton, D. R., Wieland, S. F., Uprichard, S. L., Wakita, T. & Chisari, F. V. (2005). Robust hepatitis C virus infection *in vitro*. *Proc Natl Acad Sci U S A* **102**, 9294–9299.

HEPATOLOGY
Official Journal of the American Association for the Study of Liver Diseases

Development of Hepatitis C Virus Genotype 3a Cell Culture System

Sulyi Kim,[1] Tomoko Date,[1] Hiroshi Yokokawa,[1,2] Tamaki Kono,[1] Hideki Aizaki,[1] Patrick Maurel,[3] Claire Gondeau,[3,4] and Takaji Wakita[1]

Hepatitis C virus (HCV) genotype 3a infection poses a serious health problem worldwide. A significant association has been reported between HCV genotype 3a infections and hepatic steatosis. Nevertheless, virological characterization of genotype 3a HCV is delayed due to the lack of appropriate virus cell culture systems. In the present study, we established the first infectious genotype 3a HCV system by introducing adaptive mutations into the S310 strain. HCV core proteins had different locations in JFH-1 and S310 virus-infected cells. Furthermore, the lipid content in S310 virus-infected cells was higher than Huh7.5.1 cells and JFH-1 virus-infected cells as determined by the lipid droplet staining area. *Conclusion*: This genotype 3a infectious cell culture system may be a useful experimental model for studying genotype 3a viral life cycles, molecular mechanisms of pathogenesis, and genotype 3a-specific antiviral drug development. (HEPATOLOGY 2014;60:1838-1850)

See Editorial on Page 1806

About 170 million people worldwide are infected with hepatitis C virus (HCV), which causes chronic liver disease at a high rate, leading to complications including endstage liver disease, liver cirrhosis, and hepatocellular carcinoma.[1] HCV is classified into seven major genotypes.[2] Genotype 1b is the most prevalent HCV genotype in Asian countries, followed by genotype 3a. Genotype 3a infections are more prevalent in South Asian countries with large populations.[3,4] A high incidence of hepatic steatosis is associated with genotype 3a infection.[5-7] Interferon and ribavirin combination therapy is not satisfactory in genotype 3a-infected patients, although it is more effective than in genotype 1b-infected patients.[5] The recently developed protease inhibitors telaprevir and boceprevir are also less effective against genotype 3a infection.[8] New antiviral drug development against genotype 3a HCV is necessary to improve treatment efficiency in genotype 3a-infected patients.

HCV subgenomic replicon systems are useful tools for the study of viral replication mechanisms and antiviral drug development. Recently, genotype 3a replicon systems were established.[9,10] The S310 replicon with adaptive mutations replicated efficiently in cell culture. Genotype 3a infections have a different pathogenesis as compared to other genotype infections (for example, steatosis). Previous studies demonstrated that cells expressing genotype 3a core protein had increased lipid accumulation.[11-13] Therefore, an efficient infectious viral system recapitulating the full life cycle is now essential to determine the precise pathogenesis of genotype 3a infection.

In the present study, we established an infectious genotype 3a HCV cell culture system by using S310 strains. The full-length S310 clones replicated efficiently and produced infectious viral particles. There were different HCV core localization patterns between genotype 3a S310- and genotype 2a JFH-1-infected cells. Interestingly, the lipid content in S310 virus-infected cells was higher than Huh7.5.1 cells and JFH-1 virus-infected cells as determined by lipid droplet staining area. This cell culture system will be very

Abbreviations: DMEM, Dulbecco's Modified Eagle Medium; HCV, hepatitis C virus; IgG, immunoglobulin G; LD, lipid droplet; MOI, multiplicity of infection; RT-PCR, reverse-transcriptase polymerase chain reaction; SGR, subgenomic replicon.

From the [1]Department of Virology II, National Institute of Infectious Diseases, Tokyo, Japan; [2]Pharmaceutical Research Laboratories, Toray Industries, Inc., Kanagawa, Japan; [3]Inserm U1040, Biotherapy Research Institute, Montpellier, France; [4]Department of Hepato-gastroenterology A, Hospital Saint Eloi, CHU Montpellier, France.

Received November 28, 2013; accepted April 29, 2014.

Additional Supporting Information may be found at onlinelibrary.wiley.com/doi/10.1002/hep.27197/suppinfo.

Supported by Grants-in-Aid for Scientific Research from the Japan Society for the Promotion of Science, from the Ministry of Health, Labour and Welfare of Japan, from the Ministry of Education, Culture, Sports, Science and Technology of Japan, and from the Research on Health Sciences Focusing on Drug Innovation from the Japan Health Sciences Foundation.

useful for the study of viral life cycles, molecular mechanisms of pathogenesis, and specific antiviral drug development for genotype 3a HCV.

Materials and Methods

Details of the procedures are described in the Supporting Information.

Cell Culture. HuH-7 cells (obtained from Dr. Francis V. Chisari, Scripps Research Institute California) and a derivative cell line, Huh7.5.1 cells (obtained from Dr. Francis V. Chisari) were cultured as described in the Supporting Information.

HCV Plasmid Construction. Plasmids used in the analysis were constructed based on pS310 (S310/A, DDBJ/EMBL/GenBank accession number: AB691595).[9] We constructed the full-length adapted pS310 by introducing the adaptive mutations from the SGR-S310 replicon assay. pJ6/JFH1 was previously obtained from pJFH1 by replacement with the 5′ untranslated region (UTR) to p7 region (EcoRI-BclI) of the J6CF strain (a kind gift from Dr. Jens Bukh).[14] pS310/JFH1 (constructed by Dr. Mohsan Saeed) was obtained from pJFH1 by replacement with the core to NS2 C3 junction of the pS310 strain.[15] pS310/JFH1 thus included nucleotide (nt) 1 to 2892 (amino acid [aa] 1 to 851) of S310 and nt 2888 to 9678 (aa 850 to 3033) of JFH-1 (accession number: AB047639).

RNA Synthesis and Transfection. Full-length HCV RNA was synthesized from pS310, pJFH1, pJ6/JFH1, pS310/JFH1 and the derivatives of pS310 constructs with adaptive mutations. The synthesized HCV RNA (10 μg) was transfected into Huh7.5.1 cells by electroporation, as described previously.[16-18]

Quantification of HCV Core Protein and RNA. The concentrations of HCV core protein in the culture media and cell lysates were measured by a chemiluminescent enzyme immunoassay (Lumipulse II HCV core assay, Ortho Clinical Diagnostics, Tokyo, Japan).[19] Real-time quantitative reverse-transcription polymerase chain reaction (RT-PCR) was performed to determine the copy numbers of HCV RNA as described previously.[20]

RT-PCR and Sequencing Analysis. Total RNA was extracted and purified from the culture medium or cell pellet of the HCV RNA-transfected cells. HCV cDNA was synthesized and amplified by RT-PCR as described previously.[21-23] The sequence of each amplified DNA was determined directly by using specific primers.

Determination of Infectivity. Infectivity of HCV was quantified by counting the infected foci by using fluorescence microscopy (Olympus, Tokyo, Japan), and the infectivity was expressed as the number of focus-forming units per milliliter (ffu/mL).[16,24]

Immunofluorescence Analysis and Lipid Content Quantification. Transfected or infected cells were fixed and then stained with anti-core monoclonal antibody (2H9), DAPI, and BODIPY to determine the sublocalization of core protein, nucleus, and lipid droplets (LDs), respectively. BioZero (Keyence, Tokyo, Japan) or Leica TSE SPE confocal fluorescence microscopy (Leica Microsystems, Wetzlar, Germany) were used for the observation. The LD content of cells was quantified by MetaMorph (Leica MM AF Software) analysis.[25]

Western Blot Analysis. Cell lysates were separated by sodium dodecyl sulfate-polyacrylamide gel electrophoresis (SDS-PAGE) and transferred to a PVDF membrane. HCV proteins (core, E2, and NS3) and host proteins were detected by specific antibodies.

Sucrose Density Gradient Analysis. Culture medium derived from the transfected cells was analyzed by sucrose gradient ultracentrifugation analysis.

Anti-HCV Drug Treatment. HCV-infected cells were tested with various concentrations of interferon α (IFNα, MSD K.K., Tokyo, Japan), the NS3 protease inhibitor VX-950 (Selleck Chemicals, Houston, TX), the NS5A inhibitor BMS-790052 (Selleck Chemicals), an immunosuppressant cyclosporin A (CsA, Sigma, St. Louis, MO) or the NS5B polymerase inhibitors JTK-109 (Japan Tobacco, Osaka, Japan) and PSI-6130 (Pharmasset, Princeton, NJ). After a 72-hour incubation the culture media were harvested and HCV core protein levels were quantified.

Statistical Analysis. Results were obtained from at least three independent experiments. Data are expressed as the mean ± SD. Statistical analysis was performed using Welch's t-test. $P < 0.05$ was considered statistically significant.

Address reprint requests to: Takaji Wakita, M.D., Ph.D., Department of Virology II, National Institute of Infectious Diseases, 1-23-1 Toyama, Shinjuku, Tokyo 162-8640, Japan. E-mail: wakita@nih.go.jp; fax: +81-3-5285-1161.

View this article online at wileyonlinelibrary.com.

DOI 10.1002/hep.27197

Potential conflict of interest: Nothing to report.

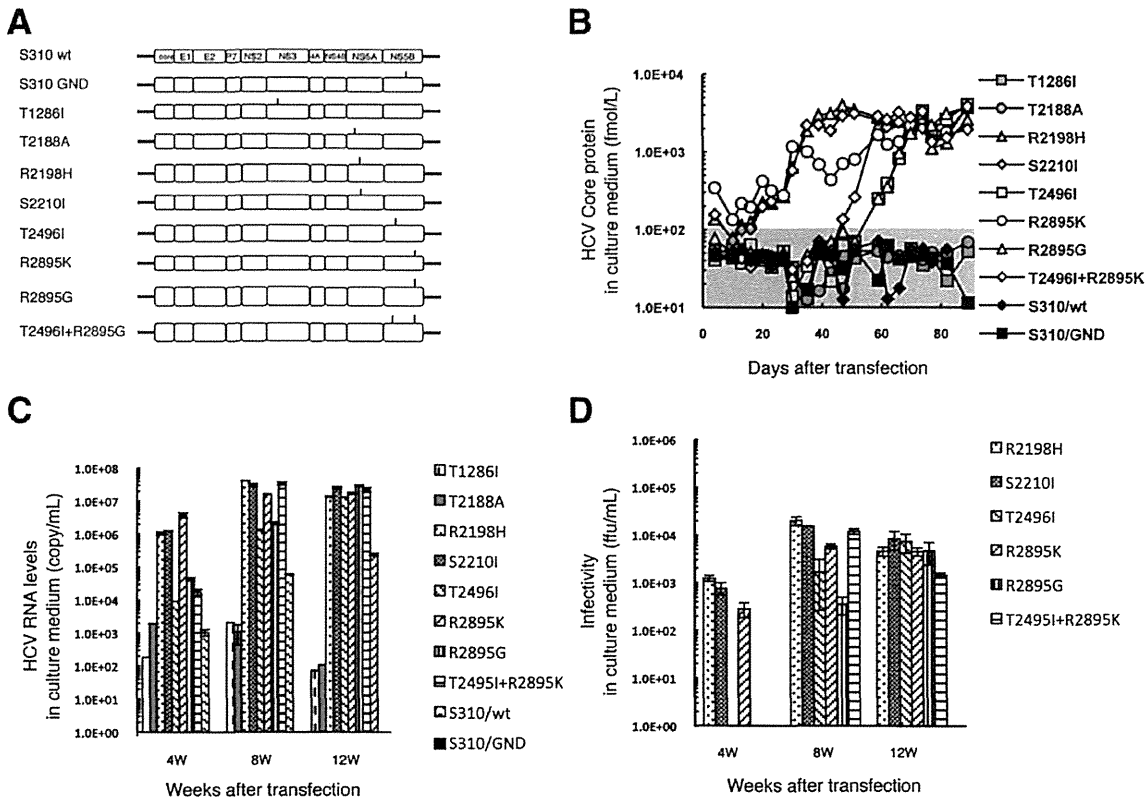

Fig. 1. Structure of full-length adapted S310 constructs and long-term culture of full-length adapted S310 clones. (A) Each mutation from subgenomic replicon clones was introduced into full-length wild-type S310. The position of each mutation is indicated by vertical lines. (B) Huh7.5.1 cells were transfected with the transcribed RNA from each construct. The cells were passaged every 3-5 days and HCV core protein levels in the culture medium at each passage were determined. Gray zone (<100 fmol/L) indicates the value below the detection limit, which was determined by mean ± 3 SD of the detection values of control culture media. (C) RNAs in the culture medium were isolated. Copy numbers of HCV RNA were determined by real-time detection RT-PCR. The culture medium at 4, 8, and 12 weeks after transfection was used. (D) Infectious titers in the culture medium were determined by focus formation assay. (E) Each passaged cell was seeded onto a slide glass. The cells were fixed, probed with the core specific antibody (green) or DAPI for nucleus staining (blue), and examined by confocal microscopy. The cells at 4, 8, and 12 weeks after transfection are shown. (F) Western blot analysis. Cell lysates were prepared from S310 clones (1; R2198H, 2; S2210I, 3; T2496I, 4; R2895K, 5; R2895G, 6; T2495I+R2895K), Huh7.5.1 cells (7), JFH-1-infected cells (8), and J6/JFH1-infected cells (9). Protein (20 μg) was separated by 12.5% SDS-PAGE, and each protein was detected by core, E2, NS3, beta actin, and GAPDH antibody. Arrows indicate the position of each protein. All assays were performed in triplicate, and data are presented as means ± standard deviation.

Results

Full-Length Constructs With Adaptive Mutations. In our previous study, several adaptive mutations were found in the genotype 3a S310 subgenomic replicon assay.[9] Those mutations were T1286I (NS3), T2188A (NS5A), R2198H (NS5A), S2210I (NS5A), T2496I (NS5B), R2895K (NS5B), R2895G (NS5B), and T2496I (NS5B) + R2895G (NS5B). We introduced these mutations into full-length S310 wild-type constructs (Fig. 1A).

Full-Length HCV Replication and Viral Production in Long-Term Culture. Viral RNA was synthesized from the full-length S310 wild- and mutant-type constructs and transfected into Huh7.5.1 cells. To examine whether these S310 constructs with adaptive mutations could continuously produce infectious virus, transfected cells were serially passaged and secreted HCV core protein levels in the culture medium were monitored (Fig. 1B). After RNA transfection, the HCV core protein levels of three mutant-type S310 constructs (R2198H, S2210I, and R2895K) continuously increased, and finally they plateaued at ~2,000-4,000 fmol/L. Interestingly, from 6-8 weeks after transfection the HCV core protein levels of the other three clones with different adaptive mutations (T2496I, R2895G, and T2496I + R2896K) increased rapidly, and their core protein levels also reached the same levels as the former three clones (R2198H, R2210I, and R2895K). Two other mutant-type (T1286I, T2188A) and wild-type S310 constructs as well as replication-incompetent mutant S310/GND

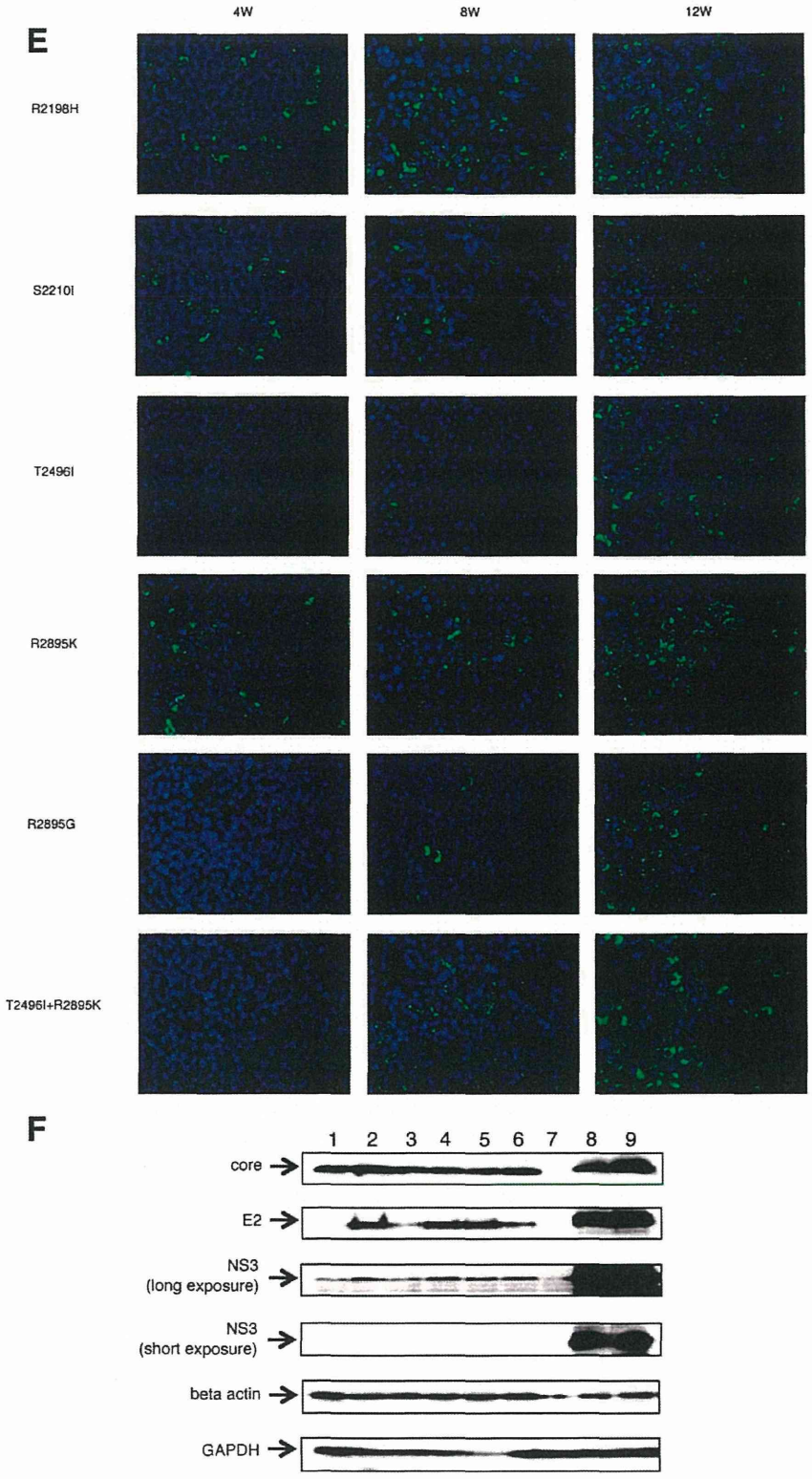

Fig. 1. (Continued)

did not secrete any HCV core protein during the observation period. We also determined the HCV RNA levels and infectivity in the culture medium at 4, 8, and 12 weeks after transfection (Fig. 1C,D). The three clones with adaptive mutations (R2198H, R2210I, and R2895K) had higher HCV RNA levels and infectivity than the other clones at 4 weeks after transfection, and their levels increased at 8 and 12 weeks after transfection. The other three clones (T2496I, R2895G, and T2496I + R2896K) had lower levels of HCV RNA and infectivity at 4 weeks after transfection, but from 8 weeks after transfection their levels were similar to the levels of the former three clones. To analyze the mechanism of this discrepancy, we determined the sequences of culture medium of six S310 clones 82 days after transfection (D82) (Table 1). Interestingly, two clones (S2210I and R2895K) that started to secrete infectious virus at earlier timepoints did not have amino acid mutations. R2198H also started to secrete infectious virus at earlier timepoints, although the virus genome had mutations in the E2 and NS3 regions (Table 1). These mutations may be necessary to produce infectious virus in this clone, but we found different mutations in the R2198H virus in an independent repeated experiment (data not shown). The virus genomes of the three other clones (T2496I, R2895G, and T2496I + R2896K) had several mutations in the E2, NS3, NS4B, NS5a, or NS5B regions (Table 1).

Table 1. Sequence Analysis and Neutralization With AP33 Antibody of Culture Medium of 82 Days After Transfection

S310 Clone	Amino Acid Mutations	Regions	AP33 IC_{50} (μg/mL)
R2198H	T416A	E2	0.0514
	H579R	E2	
	A1071V	NS3	
	K1412Q	NS3	
	H1967N	NS4B	
S2210I	ND	-	0.0472
T2496I	T416S	E2	0.0642
	A1071V	NS3	
	D1281N	NS3	
	V1756L	NS4B	
	R2895K	NS5B	
R2895K	ND	-	0.0747
R2895G	I1817V	NS4B	0.0615
	G2895A	NS5B	
	T2999S	NS5B	
T2496I + R2985K	T416N	E2	0.0413
	G2326A	NS5A	
	S2357L	NS5A	
	C2429R	NS5A	

ND, not detected.

To examine whether the replicating virus in the transfected cells could spread to the surrounding cells, the passaged transfected cells were immunostained with anti-core monoclonal antibody (Fig. 1E). We found a greater number of positive cells in three of the clones (R2198H, R2210I, and R2895K), even at 4 weeks after transfection, compared to the others, and the numbers of positive cells increased at 8 and 12 weeks after transfection. On the other hand, the other three clones (T2496I, R2895G, and T2496I + R2896K) began to get more infected at a later timepoint (8 weeks after transfection), and they showed similar numbers of positive cells at 12 weeks after transfection.

Viral protein expression in the S310-transfected cells was detected by western blotting (Fig. 1F). The core protein expression levels were similar in S310 RNA-transfected cells as compared with JFH-1 and J6/JFH1. However, E2 and NS3 protein expression levels were lower than for JFH-1 and J6/JFH1, probably due to the lower affinity of these antibodies to genotype 3a virus. We failed to detect any other NS proteins with the available antibodies. Interestingly, lower E2 protein expression levels were found in lanes 1, 3, and 6 than in the other lanes, although there were no such differences in core protein expression levels. By the sequencing analysis of the virus genome, R2198H, T2496I, and T2496I + R2895K, which had the weaker E2 signals in western blotting, each had a nonsynonymous substitution at amino acid position 416 (R2198H; T to A, T2496I; T to S, T2496I + R2895G; T to N, respectively). This position is located in the epitope of AP33, the anti-E2 antibody. The other three clones (S2210I, R2895K, and R2895G) did not have mutations in the E2 region. Therefore, it appeared that the E2 mutations might disturb antibody binding to E2 protein. To confirm whether neutralization of AP33 was affected by T416 mutations, we determined the 50% inhibitory concentrations (IC_{50}) of AP33 neutralization for each mutant virus clone. However, all clones had similar IC_{50} values (Table 1). Thus, mutations in the anti-E2 antibody epitope region influenced the results of the western blotting assay but not the neutralization assay.

To examine the viral replication and production levels at the late stage of the long-term culture, the HCV core protein levels, RNA levels, and infectivity of the cell culture medium collected 82 days after transfection were determined (Table 2). HCV core protein levels, RNA levels, and infectivity of the six S310 clones were at approximately one-tenth of the levels of the JFH-1 wild-type virus. However, these levels of infectivity (~1,000-6,000 ffu/mL) might be sufficient to maintain secreted S310 virus production and

Table 2. Quantification of HCV Core Protein Level, RNA Level, and Infectivity of Culture Medium of 82 Days After Transfection

Mutations	Core (fmol/L)	RNA (copy/mL)	Infectivity (ffu/mL)
R2198H	2,652	1.80 E+07	1,000
S2210I	3,334	8.80 E+07	4,167
T2496I	3,496	4.33 E+07	2,708
R2895K	4,716	7.83 E+07	6,042
R2895G	1,763	4.11 E+07	417
T2496I+R2895K	2,728	6.26 E+07	1,806
JFH-1	20,932	3.34 E+08	34,722
J6/JFH1	83,388	2.08 E+08	72,917

replication, since S310 clones could continuously produce the infectious virus in long-term culture (Fig. 1).

Characterization of Cell Culture-Adapted S310 Virus. To characterize the secreted infectious viral particles, we analyzed the culture medium of four S310 clones (R2198H, S2210I, R2895K, and T2496I + R2895K) by sucrose density gradient centrifugation. HCV particles produced in cell culture with the S310 clones showed major peaks of HCV core protein, RNA, and infectivity at 1.15 mg/mL (Fig. 2). JFH-1 also exhibited similar profiles of HCV core proteins and RNA, but the peak infectivity titers were usually located in a lighter fraction.[18,26] The locations of the peak infectivity titers of S310 clones were different from JFH-1.

S310 viruses (D82), JFH-1 wild-type virus, and J6/JFH1 virus were inoculated into Huh7.5.1 cells at a multiplicity of infection (MOI) of 0.3. To determine whether the cells were successfully infected, we determined and compared the intracellular and extracellular core protein levels of S310 viruses with JFH-1 and J6/JFH1 virus at 24, 48, and 72 hours after infection. Both the intracellular and extracellular core protein levels of all S310 viruses were similar to the levels of JFH-1 wild-type virus, but lower than the levels of J6/JFH1 chimeric virus (Fig. 3A,B). We also evaluated HCV RNA levels and obtained similar results with HCV core protein levels (data not shown).

Next, we determined the neutralization of the infection of these viruses by using anti-CD81 antibody (JS81). Anti-CD81 antibody treatment inhibited the infection of Huh7.5.1 cells by ~99% as compared to control IgG (Fig. 3C,D). S310 virus infection was also inhibited by AP33 anti-E2 antibody (Table 1). It is thus suggested that the S310 viruses utilize similar

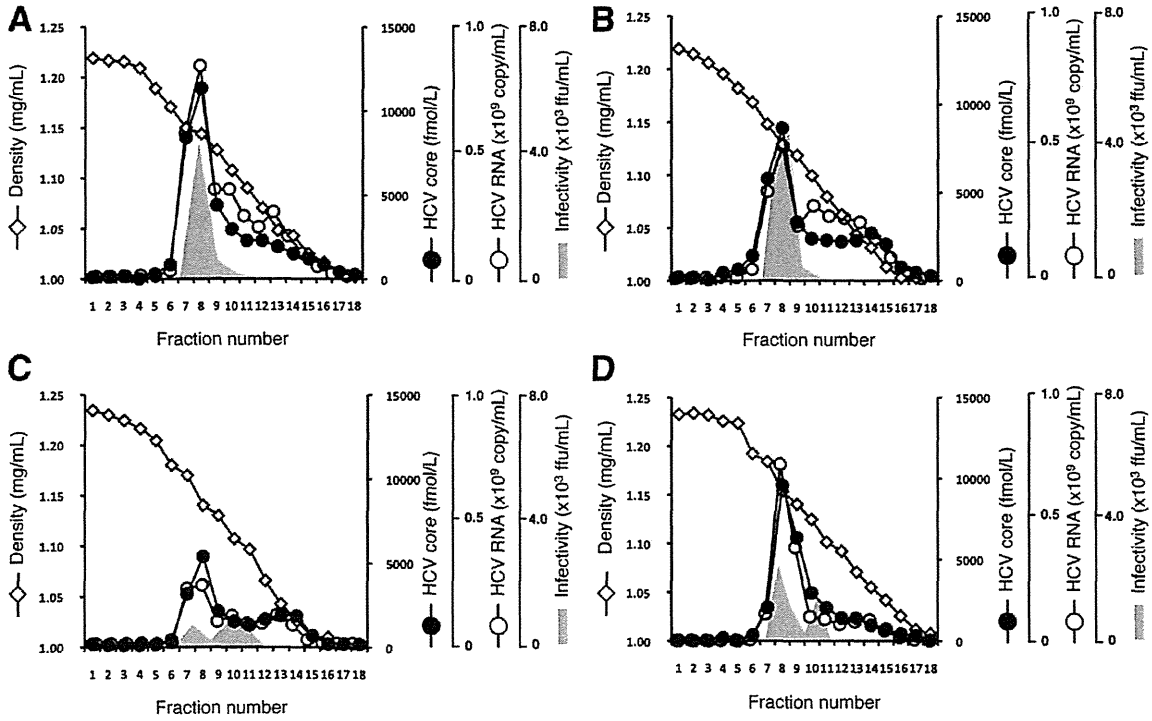

Fig. 2. Sucrose density gradient analysis of the culture medium at 8 weeks after transfection. (A) R2198H, (B) S2210I, (C) R2895K, (D) T2496I+R2895K. Culture medium was overlaid on the stepwise sucrose density gradient (0%, 10%, 20%, 30%, 40%, 50%, and 60% sucrose) and centrifuged for 18 hours at 35,000g at 4°C. A total of 18 fractions were collected from the bottom of the tubes, and density, HCV core protein level, HCV RNA level, and infectivity in each fraction were determined.

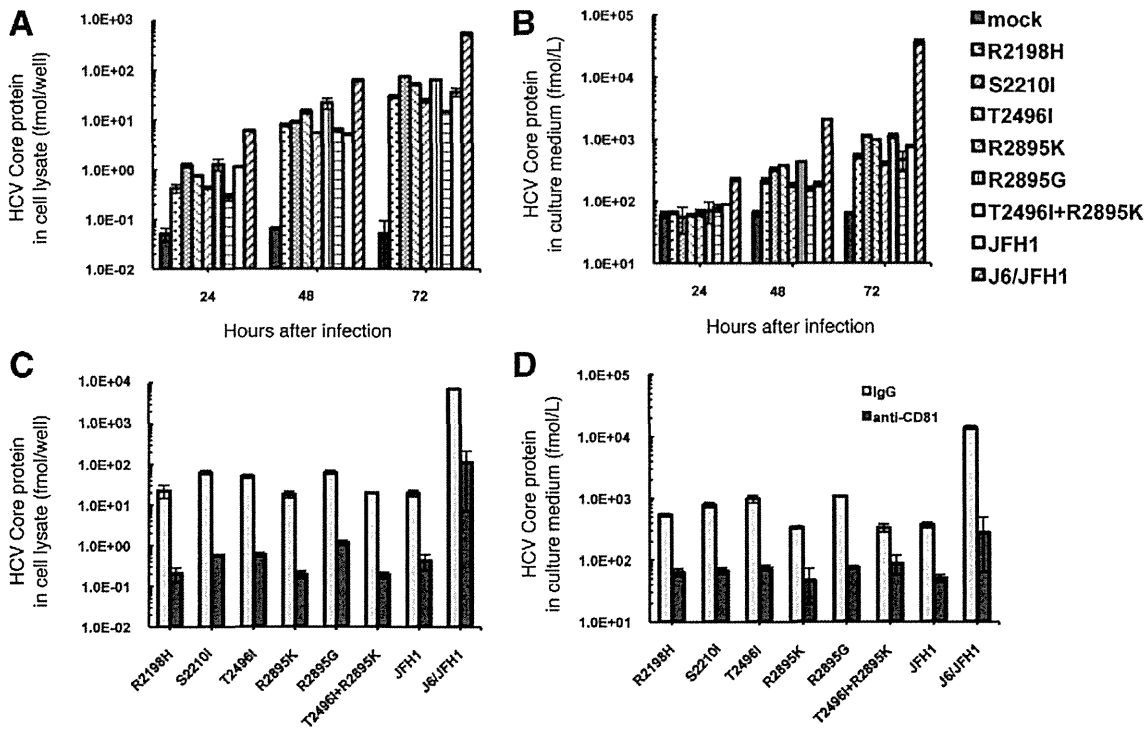

Fig. 3. Comparative analysis with the S310 viruses, JFH-1 and J6/JFH1. (A), (B) Huh7.5.1 cells were infected with the S310 viruses, JFH-1 and J6/JFH1, at an MOI of 0.3. HCV core protein levels in the cell lysate (A) and culture medium (B) were measured at 24, 48, and 72 hours after infection. (C,D) Infection with the adapted S310, JFH-1, and J6/JFH1 virus particles was inhibited by adding anti-CD81 antibody. IgG: normal human immunoglobulin G, anti-CD81: monoclonal anti-CD81 antibody. All assays were performed in triplicate, and data are presented as means ± standard deviation.

infection pathways as JFH-1 and J6/JFH1 chimeric virus, at least with respect to CD81.

To clarify the pathogenesis of genotype 3a infection, cellular sublocalization of HCV core protein and LDs in the S310-infected cells was performed with confocal microscopy. We synthesized RNA of three S310 clones (R2198H, S2210I, and R2895K), S310/JFH1 chimera, and JFH-1 and transfected the synthesized RNA into Huh7.5.1 cells. The cells were passaged every 3-5 days, and passaged cells were seeded onto a slide glass. We used BODIPY, a marker for LDs. S310-derived core proteins showed punctate patterns instead of ring-like patterns and were mainly found in the cytoplasm (Fig. 4A). S310-derived core proteins were not located around the LDs. By contrast, in the JFH-1 virus-infected cells, core proteins colocalized with LDs and exhibited ring-like patterns corresponding to the surfaces of LDs, as previously reported (Fig. 4A).[27] To confirm the intracellular localizations of HCV core protein and LDs, we magnified a partial area of each image and displayed the intensity of both fluorescences (Fig. 4B). We selected the representative region of interest (ROI1) and drew a line in each image. Intensity profiles along the line are shown on the right of the images, and red and green lines indicate the fluorescence intensities of HCV core protein and LDs, respectively. Figure 4B demonstrates that S310-derived core proteins were localized in the cytoplasm and not around the LDs, whereas JFH-1-derived core proteins were colocalized around the surfaces of LDs. These results suggest that the virus particle production pathway may be different between S310 and JFH-1 viruses.

Next, we quantified the lipid content in the infected cells. JFH-1 wild-type virus, S310 viruses (S2210I, T2496I, and R2895K) and S310/JFH1 chimeric virus were inoculated into Huh7.5.1 cell cultures at an MOI of 0.2. Inoculated cells and Huh7.5.1 cells were passaged every 3-5 days. After 11 times of serial passages, core protein, LDs, and nuclei were visualized in the cells. Representative cell images are shown in Fig. 5A. Core proteins (red) were more strongly stained in JFH-1 and S310/JFH1 virus-infected cells than in S310 virus-infected cells, and no core protein staining was observed in Huh7.5.1 cells. The LD staining (green) in the virus-infected cells was higher than in

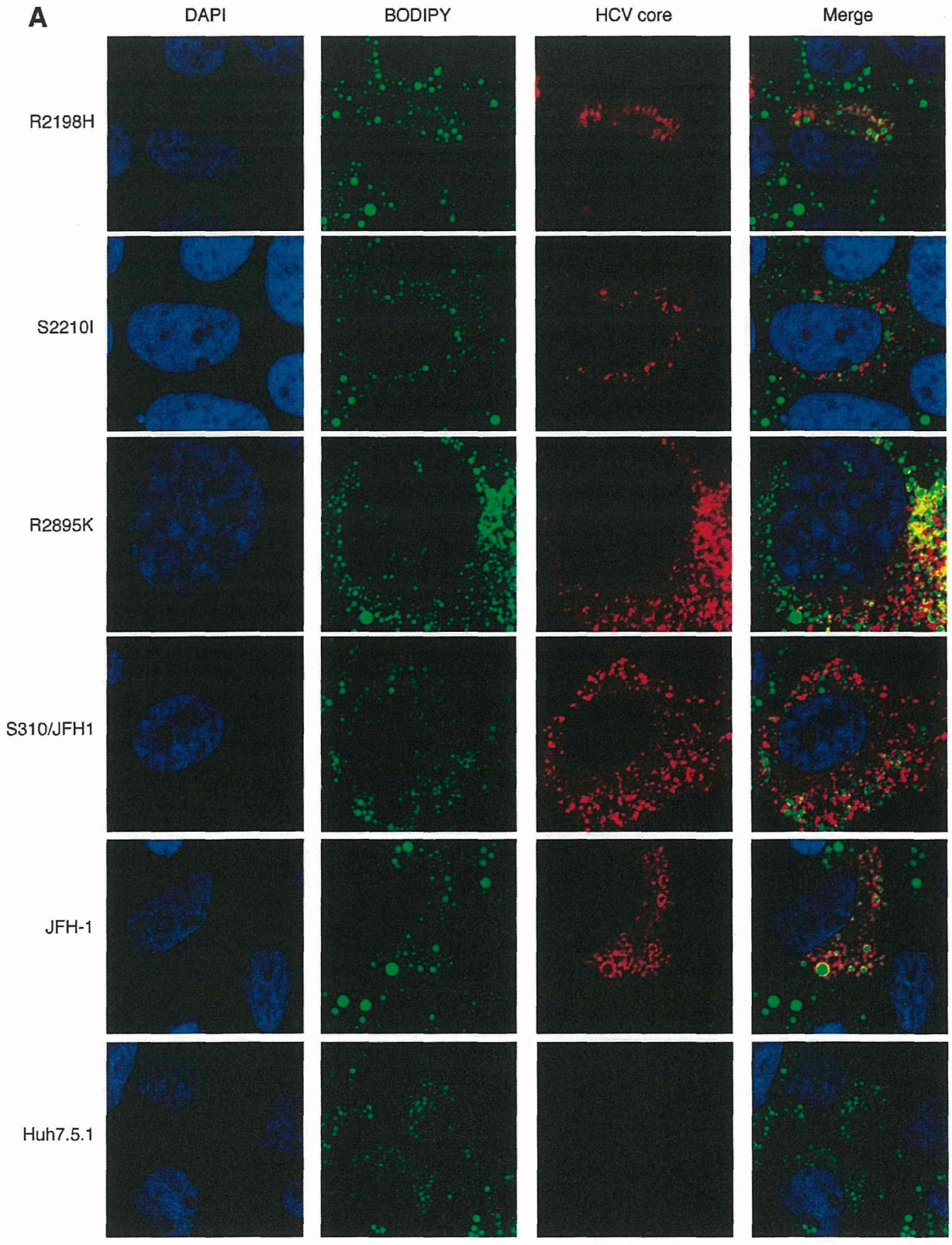

Fig. 4. Localization of HCV core proteins and lipid droplets. (A) Huh7.5.1 cells were transfected with the transcribed RNA from each construct. The cells were passaged every 3-5 days, and passaged cells were seeded onto a slide glass. The cells were fixed, probed with the core-specific antibody (red), BODIPY for lipid droplets (green), and DAPI for nucleus staining (blue), and examined by confocal microscopy. Cells at 61 days after transfection are shown. (B) Each merged image was magnified and a line was drawn across the region of interest (ROI1). Intensity profiles along the line are shown on the right of the images. The red line indicates the fluorescence intensity of HCV core protein, and the green line indicates the fluorescence intensity of LDs. The *y*-axis indicates arbitrary units of fluorescence intensity.

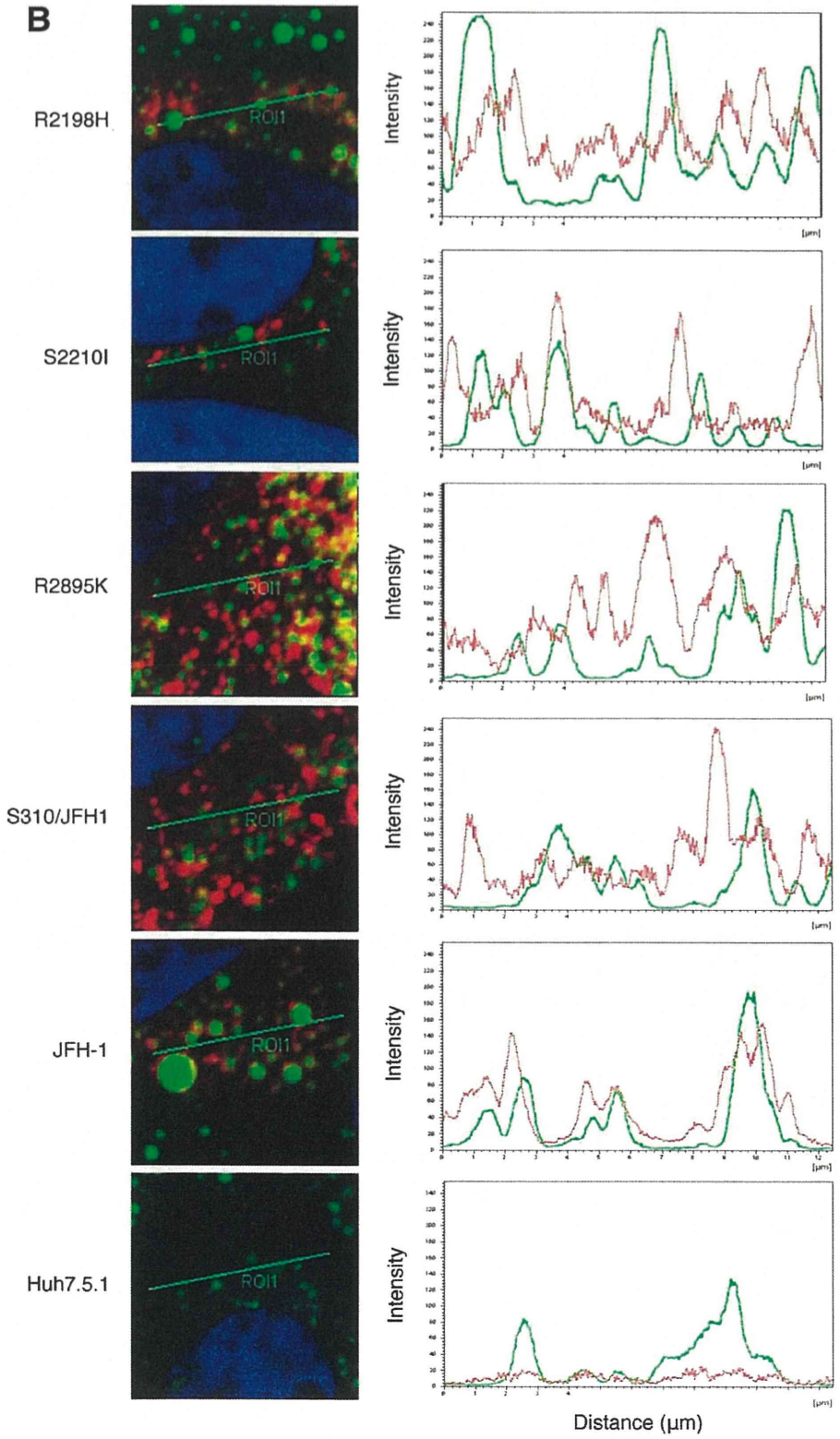

Fig. 4. (Continued)

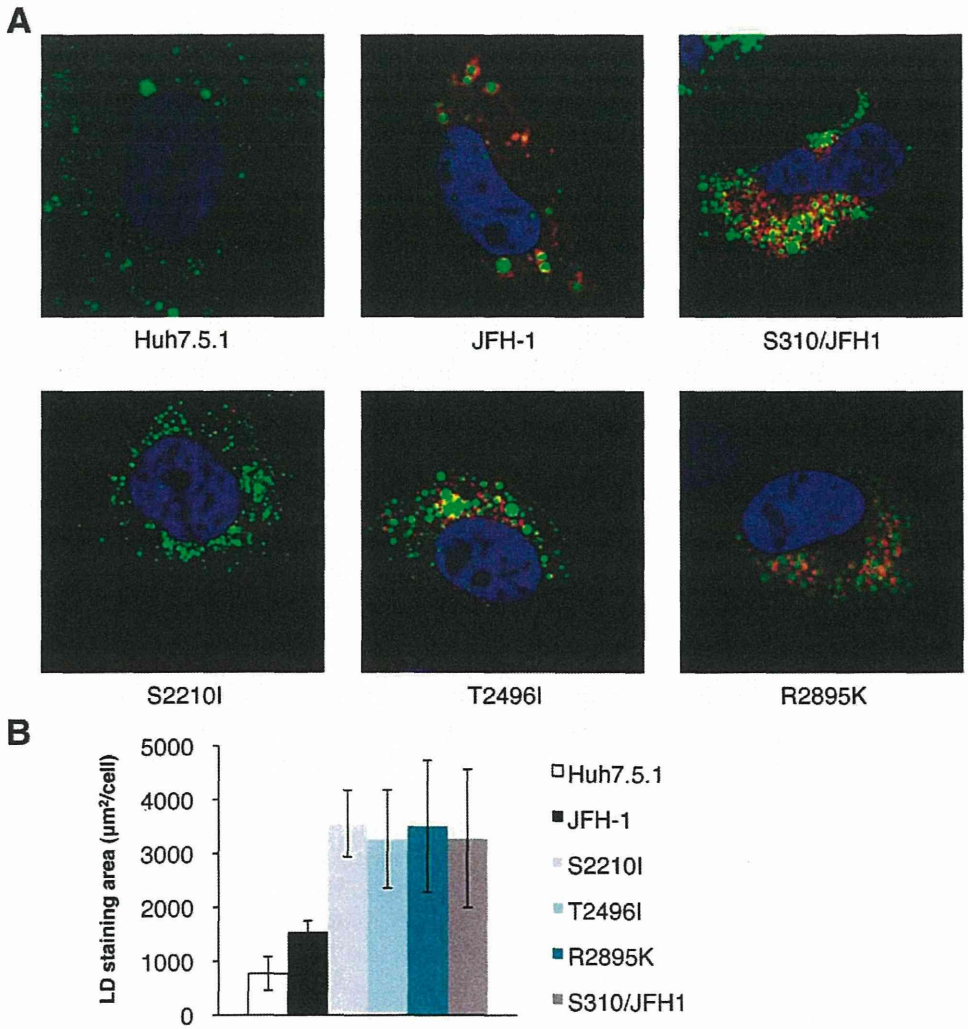

Fig. 5. Quantification of the LD content in cells. (A) Huh7.5.1 cells were inoculated with S310 viruses and JFH-1 wild-type virus at an MOI of 0.2. After 11 serial passages, the cells were analyzed as described in the Fig. 4A legend. (B) The mean values of the LD staining area in 7 cells (from Huh7.5.1 cells and JFH-1 infected cells) or 11 cells (from S310 and S310/JFH1 infected cells) were measured by MetaMorph analysis for each Huh7.5.1 cells and virus-infected cell. The *y*-axis indicates LD staining area. Mean values ± standard deviations are shown.

Huh7.5.1 cells. Furthermore, the LD staining area in the S310 virus (S2210I, T2496I, and R2895K)- and S310/JFH1-infected cells was further greater than in JFH-1-infected cells (Fig. 5A). For the statistical analysis, we selected representative similar sized cells and measured the LD staining area in a single cell by MetaMorph analysis. We analyzed seven cell images each from Huh7.5.1 cells and JFH-1, and 11 cell images each from S310/JFH1 and S310 virus-infected cells. JFH-1 infected cells exhibited significantly higher LD staining levels than Huh7.5.1 cells ($P < 0.0005$). S310 virus and S310/JFH1 chimeric virus-infected cells exhibited significantly much higher LD staining levels than Huh7.5.1 cells ($P < 0.0001$) and than JFH-1 infected cells ($P < 0.005$).

Antiviral Drug Activities Against S310 Viruses. We tested several antiviral drugs against S310 (genotype 3a) and JFH-1 (genotype 2a) infections. In the preliminary experiments, secreted HCV core protein levels were detected in parallel with intracellular HCV RNA levels. We thus used the secreted HCV core protein level as a marker of antiviral activity and determined IC_{50} values against HCV replication (Table 3). Huh7.5.1 cells were inoculated with S310 and JFH-1 viruses at an MOI of 0.2 with or without NS3 protease inhibitor (VX-950), nucleoside polymerase inhibitor (PSI-6130), nonnucleoside polymerase inhibitor (JTK-109), NS5A inhibitor (BMS-790052), CsA, and IFNα. We selected the three S310 viruses (S2210I, T2496I, and R2895K) with NS3, NS5A, or

Table 3. Antiviral Drug Activities Against HCV Infection

	VX-950 (nM)	BMS-790052 (pM)	PSI-6130 (μM)	JTK-109 (μM)	CsA (μM)	IFN-α (IU/mL)
JFH-1	31.2 ± 18.7	20.0 ± 16.8	3.4 ± 1.7	8.7 ± 2.1	0.5 ± 0.2	0.1 ± 0.1
S2210I	9841.0 ± 1026.1	48.1 ± 59.1	1.4 ± 0.1	0.7 ± 0.1*	0.2 ± 0.1	4.2 ± 4.0
T2496I	436.6 ± 81.7*	24.4 ± 23.4	5.6 ± 5.2	2.3 ± 0.6*	0.7 ± 0.6	0.2 ± 0.2
R2895K	436.3 ± 249.8	10.2 ± 1.7	1.6 ± 0.2	1.4 ± 1.2*	0.9 ± 0.8	4.6 ± 3.7

Assays were performed in triplicate and IC_{50} values are expressed as mean ± standard deviations.
*$P < 0.05$ versus JFH-1.

NS5B adaptive mutations (Table 1). In VX-950 treatment, IC_{50} values for S310 infection seemed to be higher than for JFH-1 infection; however, a statistically significant increase was only observed with T2496I virus infection as compared to JFH-1 virus infection (Table 3). This lack of significance may be due to the large experimental deviation in other S310 virus infections. PSI-6130 inhibited both genotype virus infections at similar levels. However, JTK-109 was significantly more effective against S310 viruses than JFH-1 virus ($P < 0.05$). BMS-790052, CsA, and IFNα inhibited both JFH-1 and S310 viruses at similar levels. There were no differences in antiviral drug efficacies among S310 clones except for VX-950. Adaptive mutations in these three clones may not be important for drug efficacies. Cell viability was determined by the WST-1 assay, and there was no cellular toxicity within the tested dose of the drugs (data not shown).

Discussion

In the present study, we established a cell-culture-adapted genotype 3a infectious virus system. In a previous study, adaptive mutations were important for efficient replication of a genotype 3a subgenomic replicon (S310).[9] Therefore, we introduced these mutations into full-length S310 constructs to determine if these constructs can replicate and produce infectious virus particles in cell culture. Full-length S310 wild-type virus did not exhibit increased intracellular and extracellular core levels. However, some of the full-length S310 viruses with adaptive mutations displayed increased intracellular and extracellular core levels in a transient virus production assay (data not shown). To examine whether these clones could continuously produce infectious viral particles, we passaged the S310 RNA-transfected cells repeatedly and monitored the HCV core protein levels in the culture medium for 3 months. As a result, HCV core protein levels of the three clones with adaptive mutations (R2198H, S2210I, and R2895K) increased soon after the transfection and eventually plateaued. From 6 to 8 weeks after transfection, extracellular HCV core protein levels of the other three clones with adaptive mutations (T2496I, R2895G, and T2496I + R2896K) increased rapidly, and their extracellular core protein levels also reached levels similar to the former three clones. All six clones showed sufficient viral RNA replication, virus production, and infectivity for autonomous virus expansion at the end of culture (D82). By sucrose density gradient analysis, we confirmed that S310 clones exhibited similar profiles of HCV core protein and RNA to JFH-1, but the peak infectivity titers were located in the same fraction as HCV core proteins and RNA. The peak infectivity of S310 clones shifted to the heavier fractions as compared to JFH-1. In a previous study, it was also reported that a particular mutant JFH-1 strain exhibited both HCV RNA and infectivity in the same fraction.[28] In that study, a point mutation (G451R) was identified in the viral E2 protein, and the G451R mutation was speculated to increase the density and infectivity of the virus particles.[29] It is thus possible that E2 proteins of S310 clones also alter the density of infectious viral particles. Upon inoculation of secreted S310 viruses into naïve Huh7.5.1 cells, both intracellular and extracellular core protein levels of infected cells were at levels similar to JFH-1 but less than J6/JFH1. In the neutralization experiment, S310 infections of Huh7.5.1 cells were sensitive to anti-CD81 and anti-E2 antibody treatment. Thus, these results suggest that S310 viruses can replicate efficiently and produce infectious virus particles.

Patients with genotype 3a HCV infections tend to develop hepatic steatosis, an intracellular accumulation of lipids and subsequent formation of LDs in the cytoplasm of hepatocytes.[30] S310-infected patient also showed microvesicular and macrovesicular steatosis both before and after liver transplantation. The LD is an organelle used for the storage of neutral lipids. Hepatic steatosis might be involved in inducing lipid synthesis by activation of SREBP-1 and peroxisome proliferator-activated receptor gamma (PPARγ) or by producing reactive oxygen species.[31-33] Inversely, MTP and PPARα might be involved in decreasing lipid secretion and degradation.[34,35]

In previous studies, cells expressing genotype 3a core protein were used to study the genotype 3a HCV core protein association with steatosis.[11-13] HCV genotype 3a core protein up-regulated the activity of fatty acid synthase promoter.[36] Domain 3 of the HCV core protein was sufficient for lipid accumulation, and specific polymorphisms in the HCV core protein of genotype 3a increased the lipid levels, contributing to steatosis in cultured cells.[11] However, the previous systems used only core protein expression, so they lacked the effects of other viral proteins and the entire viral life cycle. Furthermore, HCV core protein sublocalization on the LD surface is important for infectious virus particle formation.[29] We thus analyzed core protein and LD sublocalization by using the genotype 3a infection system. S310-derived core proteins showed punctate signals rather than the ring-like core protein staining pattern usually seen in JFH-1-infected cells (Fig. 4A). We further examined whether S310 infection resulted in the accumulation of LDs in a long-term culture of infected cells. Interestingly, S310 virus-infected cells exhibited greater LD accumulation than Huh7.5.1 cells and JFH-1 virus-infected cells. In addition, LD accumulation in the S310/JFH1 chimeric virus-infected cells was similar to S310 virus-infected cells. S310/JFH1 chimeric virus consists of the S310-derived structural region and the JFH-1-derived nonstructural region. The result thus suggests that the S310-derived structural region is important for LD accumulation in the S310-infected cells. To examine the gene expression levels important for cellular lipid metabolism, we examined MTP, PPARα, and SREBP-1c mRNA expression by real-time PCR. However, no differences in mRNA expression levels were found in between Huh7.5.1 cells and the infected cells (data not shown). Further detailed analysis will be necessary to clarify the mechanisms for LD accumulation in S310 virus-infected cells.

To provide new therapeutic approaches for genotype 3a HCV infections, we examined the antiviral drug activity against S310-infected cells. In VX-950 treatment, IC_{50} values for S310 infection seemed to be higher than for JFH-1 infection; however, VX-950 was only statistically less effective for T2496I infection as compared to JFH-1 infection. In our previous study, another NS3 protease inhibitor, BILN-2061, was also less effective for the S310 subgenomic replicon as compared to the JFH-1 and Con1 replicons. JTK-109, a nonnucleoside polymerase inhibitor, was more effective for S310 than JFH-1. Other inhibitors, including NS5A inhibitor, nucleoside NS5B inhibitor, IFNα, and CsA, inhibited both viruses at similar levels. Thus, this novel genotype 3a cell culture system can be used to assay possible antiviral compounds.

In conclusion, we established an HCV genotype 3a cell culture system. The patients infected with genotype 3a HCV appear to have different clinical characteristics than patients infected with other genotypes. This genotype 3a infectious cell culture system will be useful for studying the molecular mechanism of HCV viral life cycles and pathogenesis, as well as for developing specific antiviral drugs for genotype 3a infections.

Acknowledgment: Huh7.5.1 cells were kindly provided by Dr. Francis V. Chisari. The pS310/JFH1 plasmid was constructed by Dr. Mohsan Saeed. The J6CF plasmid was a kind gift from Dr. Jens Bukh. AP33 antibody was generously provided by Genentech. JTK-109 and PSI-6130 were generous gifts from Japan Tobacco, Inc., and Pharmasset, Inc., respectively.

References

1. Feld JJ, Liang TJ. Hepatitis C — identifying patients with progressive liver injury. HEPATOLOGY 2006;43:S194-206.
2. Smith DB, Bukh J, Kuiken C, Muerhoff AS, Rice CM, Stapleton JT, et al. Expanded classification of hepatitis C Virus into 7 genotypes and 67 subtypes: updated criteria and assignment web resource. HEPATOLOGY 2014;59:318-327.
3. Butt S, Idrees M, Akbar H, ur Rehman I, Awan Z, Afzal S, et al. The changing epidemiology pattern and frequency distribution of hepatitis C virus in Pakistan. Infect Genet Evol 2010;10:595-600.
4. Rehman IU, Idrees M, Ali M, Ali L, Butt S, Hussain A, et al. Hepatitis C virus genotype 3a with phylogenetically distinct origin is circulating in Pakistan. Genet Vaccines Ther 2011;9:2.
5. Hui JM, Kench J, Farrell GC, Lin R, Samarasinghe D, Liddle C, et al. Genotype-specific mechanisms for hepatic steatosis in chronic hepatitis C infection. J Gastroenterol Hepatol 2002;17:873-881.
6. Rubbia-Brandt L, Quadri R, Abid K, Giostra E, Male PJ, Mentha G, et al. Hepatocyte steatosis is a cytopathic effect of hepatitis C virus genotype 3. J Hepatol 2000;33:106-115.
7. Kumar D, Farrell GC, Fung C, George J. Hepatitis C virus genotype 3 is cytopathic to hepatocytes: reversal of hepatic steatosis after sustained therapeutic response. HEPATOLOGY 2002;36:1266-1272.
8. Gottwein JM, Scheel TK, Jensen TB, Ghanem L, Bukh J. Differential efficacy of protease inhibitors against HCV genotypes 2a, 3a, 5a, and 6a NS3/4A protease recombinant viruses. Gastroenterology 2011;141:1067-1079.
9. Saeed M, Gondeau C, Hmwe S, Yokokawa H, Date T, Suzuki T, et al. Replication of hepatitis C virus genotype 3a in cultured cells. Gastroenterology 2013;144:56-58 e57.
10. Saeed M, Scheel TK, Gottwein JM, Marukian S, Dustin LB, Bukh J, et al. Efficient replication of genotype 3a and 4a hepatitis C virus replicons in human hepatoma cells. Antimicrob Agents Chemother 2012;56:5365-5373.
11. Jhaveri R, McHutchison J, Patel K, Qiang G, Diehl AM. Specific polymorphisms in hepatitis C virus genotype 3 core protein associated with intracellular lipid accumulation. J Infect Dis 2008;197:283-291.
12. Jhaveri R, Qiang G, Diehl AM. Domain 3 of hepatitis C virus core protein is sufficient for intracellular lipid accumulation. J Infect Dis 2009;200:1781-1788.
13. Qiang G, Jhaveri R. Lipid droplet binding of hepatitis C virus core protein genotype 3. ISRN Gastroenterol 2012;2012:176728.
14. Lindenbach BD, Evans MJ, Syder AJ, Wolk B, Tellinghuisen TL, Liu CC, et al. Complete replication of hepatitis C virus in cell culture. Science 2005;309:623-626.

15. Pietschmann T, Kaul A, Koutsoudakis G, Shavinskaya A, Kallis S, Steinmann E, et al. Construction and characterization of infectious intragenotypic and intergenotypic hepatitis C virus chimeras. Proc Natl Acad Sci U S A 2006;103:7408-7413.
16. Kato T, Date T, Murayama A, Morikawa K, Akazawa D, Wakita T. Cell culture and infection system for hepatitis C virus. Nat Protoc 2006;1:2334-2339.
17. Wakita T. Isolation of JFH-1 strain and development of an HCV infection system. Methods Mol Biol 2009;510:305-327.
18. Wakita T, Pietschmann T, Kato T, Date T, Miyamoto M, Zhao Z, et al. Production of infectious hepatitis C virus in tissue culture from a cloned viral genome. Nat Med 2005;11:791-796.
19. Saeed M, Suzuki R, Kondo M, Aizaki H, Kato T, Mizuochi T, et al. Evaluation of hepatitis C virus core antigen assays in detecting recombinant viral antigens of various genotypes. J Clin Microbiol 2009;47:4141-4143.
20. Takeuchi T, Katsume A, Tanaka T, Abe A, Inoue K, Tsukiyama-Kohara K, et al. Real-time detection system for quantification of hepatitis C virus genome. Gastroenterology 1999;116:636-642.
21. Date T, Miyamoto M, Kato T, Morikawa K, Murayama A, Akazawa D, et al. An infectious and selectable full-length replicon system with hepatitis C virus JFH-1 strain. Hepatol Res 2007;37:433-443.
22. Kato T, Date T, Miyamoto M, Furusaka A, Tokushige K, Mizokami M, et al. Efficient replication of the genotype 2a hepatitis C virus subgenomic replicon. Gastroenterology 2003;125:1808-1817.
23. Date T, Kato T, Kato J, Takahashi H, Morikawa K, Akazawa D, et al. Novel cell culture-adapted genotype 2a hepatitis C virus infectious clone. J Virol 2012;86:10805-10820.
24. Zhong J, Gastaminza P, Cheng G, Kapadia S, Kato T, Burton DR, et al. Robust hepatitis C virus infection in vitro. Proc Natl Acad Sci U S A 2005;102:9294-9299.
25. Olmstead AD, Knecht W, Lazarov I, Dixit SB, Jean F. Human subtilase SKI-1/S1P is a master regulator of the HCV Lifecycle and a potential host cell target for developing indirect-acting antiviral agents. PLoS Pathog 2012;8:e1002468.
26. Kato T, Matsumura T, Heller T, Saito S, Sapp RK, Murthy K, et al. Production of infectious hepatitis C virus of various genotypes in cell cultures. J Virol 2007;81:4405-4411.
27. Miyanari Y, Atsuzawa K, Usuda N, Watashi K, Hishiki T, Zayas M, et al. The lipid droplet is an important organelle for hepatitis C virus production. Nat Cell Biol 2007;9:1089-1097.
28. Gastaminza P, Dryden KA, Boyd B, Wood MR, Law M, Yeager M, et al. Ultrastructural and biophysical characterization of hepatitis C virus particles produced in cell culture. J Virol 2010;84:10999-11009.
29. Zhong J, Gastaminza P, Chung J, Stamataki Z, Isogawa M, Cheng G, et al. Persistent hepatitis C virus infection in vitro: coevolution of virus and host. J Virol 2006;80:11082-11093.
30. Anderson N, Borlak J. Molecular mechanisms and therapeutic targets in steatosis and steatohepatitis. Pharmacol Rev 2008;60:311-357.
31. Gavrilova O, Haluzik M, Matsusue K, Cutson JJ, Johnson L, Dietz KR, et al. Liver peroxisome proliferator-activated receptor gamma contributes to hepatic steatosis, triglyceride clearance, and regulation of body fat mass. J Biol Chem 2003;278:34268-34276.
32. Videla LA, Rodrigo R, Orellana M, Fernandez V, Tapia G, Quinones L, et al. Oxidative stress-related parameters in the liver of non-alcoholic fatty liver disease patients. Clin Sci (Lond) 2004;106:261-268.
33. Ma S, Yang D, Li D, Tan Y, Tang B, Yang Y. Inhibition of uncoupling protein 2 with genipin exacerbates palmitate-induced hepatic steatosis. Lipids Health Dis 2012;11:154.
34. Perlemuter G, Sabile A, Letteron P, Vona G, Topilco A, Chretien Y, et al. Hepatitis C virus core protein inhibits microsomal triglyceride transfer protein activity and very low density lipoprotein secretion: a model of viral-related steatosis. FASEB J 2002;16:185-194.
35. Mirandola S, Realdon S, Iqbal J, Gerotto M, Dal Pero F, Bortoletto G, et al. Liver microsomal triglyceride transfer protein is involved in hepatitis C liver steatosis. Gastroenterology 2006;130:1661-1669.
36. Jackel-Cram C, Babiuk LA, Liu Q. Up-regulation of fatty acid synthase promoter by hepatitis C virus core protein: genotype-3a core has a stronger effect than genotype-1b core. J Hepatol 2007;46:999-1008.

Supporting Information

Additional Supporting Information may be found at onlinelibrary.wiley.com/doi/10.1002/hep.27197/suppinfo.

Gastroenterology 2014;147:463–472

Cyclophilin Inhibitors Reduce Phosphorylation of RNA-Dependent Protein Kinase to Restore Expression of IFN-Stimulated Genes in HCV-Infected Cells

Takuji Daito,[1,2] Koichi Watashi,[1] Ann Sluder,[2] Hirofumi Ohashi,[1] Syo Nakajima,[1] Katyna Borroto-Esoda,[2] Takashi Fujita,[3] and Takaji Wakita[1]

[1]*Department of Virology II, National Institute of Infectious Diseases, Tokyo, Japan;* [2]*SCYNEXIS, Inc, Durham, North Carolina; and* [3]*Laboratory of Molecular Genetics, Institute for Virus Research, Kyoto University, Kyoto, Japan*

BACKGROUND & AIMS: Cyclophilin inhibitors are being developed for treatment of hepatitis C virus (HCV) infection. They are believed to inhibit the HCV replication complex. We investigated whether cyclophilin inhibitors interact with interferon (IFN) signaling in cultured cells infected with HCV. **METHODS:** We used immunoblot assays to compare expression of IFN-stimulated genes (ISGs) and of components of IFN signaling in HCV-infected and uninfected cells. **RESULTS:** Incubation with IFN alfa induced expression of ISGs in noninfected cells and, to a lesser extent, in HCV-infected cells; addition of the cyclophilin inhibitor SCY-635 restored expression of ISG products in HCV-infected cells. SCY-635 reduced phosphorylation of double-strand RNA-dependent protein kinase (PKR) and its downstream factor eIF2α; the phosphorylated forms of these proteins are negative regulators of ISG translation. Cyclophilin A interacted physically with PKR; this interaction was disrupted by SCY-635. SCY-635 also suppressed PKR-mediated formation of stress granules. Cyclophilin inhibitors were found to inhibit PKR phosphorylation and stress granule formation in HCV-infected and uninfected cells. **CONCLUSIONS:** In cultured cells, cyclophilin inhibitors reverse the attenuation of the IFN response by HCV, in addition to their effects on HCV replication complex. Cyclophilin A regulation of PKR has been proposed as a mechanism for observed effects of cyclophilin inhibitors on IFN signaling. We found that cyclophilin inhibitors reduce phosphorylation of PKR and eIF2α during HCV infection to allow for translation of ISG products. Proteins in this pathway might be developed as targets for treatment of HCV infection.

Keywords: Signal Transduction; Cyclosporin; Innate Immunity; Replication.

Hepatitis C virus (HCV) infection, which affects approximately 170 million people worldwide, is a leading cause of liver cirrhosis and hepatocellular carcinoma.[1–6] The current standard anti-HCV treatment employs pegylated interferon (IFN) and ribavirin, in combination with newly approved protease inhibitors.[7–10] In addition to these clinically available drugs, a variety of anti-HCV compounds are under clinical development. Direct-acting antiviral agents that target viral proteins to suppress HCV replication include protease inhibitors, polymerase inhibitors, and NS5A inhibitors.[4,11] Host-targeting antiviral agents are alternative classes of anti-HCV candidates that act by inhibiting host factors essential for HCV replication.[3,4,11,12]

Cyclophilin (CyP) inhibitors, including alisporivir (Debio 025), NIM811, and SCY-635, are a class of host-targeting antiviral agents showing a significant anti-HCV effect in HCV-infected patients.[13] These agents target cellular CyPs, which are peptidyl prolyl cis-trans isomerases catalyzing conformational changes in proteins. The CyP family consists of >15 subtypes, including CyPA, CyPB, and CyPD.[14] We initially reported that cyclosporin A (CsA), the prototype CyP inhibitor, suppressed HCV RNA replication in the HCV subgenomic replicon system.[15–18] Subsequent studies suggested that CyPA is likely to be the main CyP acting in HCV RNA replication.[19–22] Although the precise mechanism by which CyPs regulate HCV RNA replication is still under investigation, this protein family is likely to directly regulate the function or formation of the RNA replication machinery.[13]

Interestingly, recent clinical studies of the CyP inhibitors, alisporivir and SCY-635, without IFN showed that the decline of HCV viral load after CyP inhibitor administration was likely to be influenced by interleukin (IL)28B genotype, viral load reduction was drastic in CC genotype patients, and was relatively moderate in CT and TT patients, similar to the case with IFN-based treatment.[23,24] In addition, studies with SCY-635 reported that administration of SCY-635 monotherapy up-regulated the serum levels of IFN-stimulated gene (ISG) protein products in HCV-infected patients. These data suggest that CyP inhibitors may cross talk with the IFN signaling pathway(s) in HCV-infected cells and patients.

In general, the antiviral activity of IFN alfa is mediated by downstream genes of the IFN signaling pathway, which are classified as ISGs.[25–27] IFN-alfa stimulation triggers

Abbreviations used in this paper: **CsA, cyclosporin A; CyP, cyclophilin; HCV, hepatitis C virus; IFN, interferon; IL, interleukin; ISG, IFN-stimulated gene; mRNA, messenger RNA; PKR, double-strand RNA-dependent protein kinase; SG, stress granule; STAT, signal transducers and activators of transcription.**

0016-5085/$36.00
http://dx.doi.org/10.1053/j.gastro.2014.04.035

the Janus-activated kinase/signal transducers and activators of transcription (STAT) signaling pathway, in which STAT1 and STAT2 are phosphorylated by Janus-activated kinase family proteins and then form a complex with ISGF3γ to translocate into the nucleus. The ISGF3 complex drives IFN-stimulated response element–mediated transcription to induce messenger RNA (mRNA) for ISGs, which is then translated into ISG proteins. Recently, it was reported that protein translation from mRNA for ISGs triggered by IFN, as well as for other host proteins, was negatively regulated in HCV-infected cells by the phosphorylation of double-stranded RNA-dependent protein kinase (PKR) and its downstream target eIF2α.[28–30] It was also reported that the formation of stress granules (SG) triggered by phosphorylated PKR induced translational termination of proteins, including ISGs.[29–31] However, the therapeutic relevance of this phenomenon regulated by phosphorylated PKR has not yet been demonstrated.

An understanding of the mechanisms for antiviral agents is important for predicting the antiviral efficacy, as well as providing appropriate treatment to patients. In this study, we analyzed the interaction of CyP inhibitors and the IFN signaling pathway in HCV-infected cells. CyP inhibitors restored ISG protein production in HCV-infected cells through impairment of PKR phosphorylation. CyPA was involved in the regulation of PKR phosphorylation. CyPA interacted with PKR in both HCV-infected and uninfected cells. SG formation triggered by PKR was inhibited by CyP inhibitors. These findings suggest that CyPA is a functional regulator of the IFN signaling pathway at the translational level, and that CyP inhibitors can unexpectedly exhibit a dual mechanism for their anti-HCV activity.

Materials and Methods

Materials and Methods are shown in the Supplemental Material.

Results

SCY-635 Restored Interferon-Alfa–Induced Interferon-Stimulated Gene Protein Production in Hepatitis C Virus–Infected Cells

In HCV-infected patients, ISG protein production, monitored by 2′5′ oligoadenylate synthetase–1 protein level in serum, was augmented along with SCY-635 concentration (Supplementary Figure 1) as reported previously.[23] Productions of IFN alfa and IFN gamma 1, which are also induced as ISGs,[32] were consistently increased after serum SCY-635 level (Supplementary Figure 1). These ISG protein inductions by SCY-635 treatment were not observed in noninfected healthy volunteers. These data raised the unexpected possibility that SCY-635 facilitated the production of ISG proteins upon HCV infection.

We then investigated the ISG induction triggered by IFN-alfa stimulation of HCV-infected cells. Huh-7 cells were infected with HCV JFH1 at a multiplicity of infection of 0.2 or left uninfected. After 4 days, when >70% of the cell population was HCV infected, the cells were stimulated with IFNα for 16 hours to induce ISG proteins; parallel control cultures were not treated with IFN alfa. Protein production of representative ISGs, ISG15 and MxA, but not of actin as an internal control, was increased after IFN-alfa treatment in both HCV-infected and uninfected cells (Figure 1*A*, compare *lanes 1* and *2*; *lanes 3* and *4*). However, ISG induction in HCV-infected cells was impaired compared with that in uninfected cells (Figure 1*A*, compare *lanes 2* and *4*), consistent

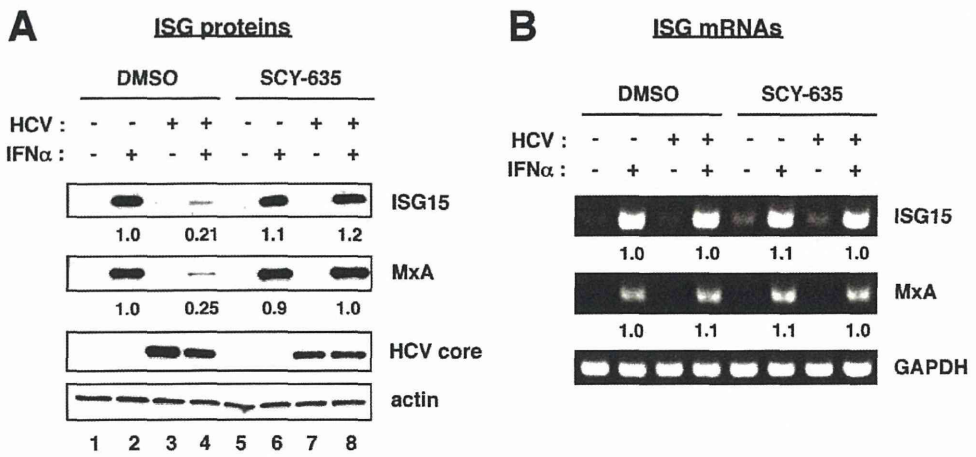

Figure 1. Protein production of ISGs in HCV-infected cells was restored by treatment with a CyP inhibitor, SCY-635. (*A*) HCV-infected (*lanes 3, 4, 7,* and *8*) or uninfected Huh-7 cells (*lanes 1, 2, 5,* and *6*) were pretreated with dimethyl sulfoxide (DMSO), 0.05% (*lanes 1–4*) or SCY-635, 2 μM (*lanes 5–8*) for 24 hours, and then treated with (*lanes 2, 4, 6, 8*) or without (*lanes 1, 3, 5, 7*) IFN alfa, 100 IU/mL for 16 hours (*A*) or 8 hours (*B*). Protein levels of ISG15, MxA, HCV core, and actin were detected by Western blot (*A*). mRNA expression levels of ISG15, MxA, and glyceraldehyde-3-phosphate dehydrogenase (GAPDH) were detected by reverse transcription polymerase chain reaction (*B*). Relative band intensities (see Materials and Methods) for these proteins and mRNAs by setting those in treatment with IFN alfa plus DMSO as 1.0 are shown below the panels. We performed 3 independent experiments for each figure in this study and obtained similar results in each replicate.

with previous observations.[29] Intriguingly, pretreatment with a CyP inhibitor, SCY-635,[23] restored the IFN-alfa–induced up-regulation of ISG protein production in HCV-infected cells (Figure 1*A*, *lane 8*). In contrast, the mRNA levels for these ISGs were not significantly changed by SCY-635 (Figure 1*B*). These results suggest that SCY-635 restores IFN-alfa–induced ISG induction in HCV-infected cells at a post-transcriptional level.

SCY-635 Inhibited the Phosphorylation of Double-Strand RNA-Dependent Protein Kinase

ISG protein production can be regulated at 2 levels, transcriptionally and post transcriptionally (see Figure 7). Stimulation of cells with type I IFNs induces phosphorylation of STAT1 and STAT2, which then form a complex with ISGF3γ that transactivates gene transcription via the IFN-stimulated response element to induce ISG mRNAs.[33] In addition, the subsequent translational level is regulated by PKR and its downstream target eIF2α.[29,30] To explore the mechanism of ISG-production restoration by SCY-635, we treated HCV-infected cells with another anti-HCV drug, telaprevir,[34] an HCV protease inhibitor, as well as SCY-635, and examined the IFN response of the treated cells. Protein production of ISG15 and ISG56 on IFN-alfa stimulation was augmented in the cells pretreated with SCY-635, however, the effect of telaprevir was less pronounced (Figure 2*Ai* and *ii*, Supplementary Figure 2 for statistics). Given that the anti-HCV effect of telaprevir was greater than that of SCY-635, as monitored by HCV core protein production (Figure 2*Avii*) and HCV RNA level (Supplementary Figure 3*A*) (50% effective concentrations of SCY-635 and telaprevir were 0.51 and 0.36 μM, respectively), these data suggest that the SCY-635 effect on ISG up-regulation was not primarily mediated by the elimination of HCV from the cells, but rather by a more direct interaction of SCY-635 with the IFN pathway. Intriguingly, SCY-635 drastically decreased the level of PKR that was phosphorylated at amino acid threonine 446, without reducing the total amount of PKR (Figure 2*Aiii, iv*). In addition, downstream phosphorylation of eIF2α was consistently inhibited by treatment with SCY-635 (Figure 2*Av*). The modest effect of telaprevir on the

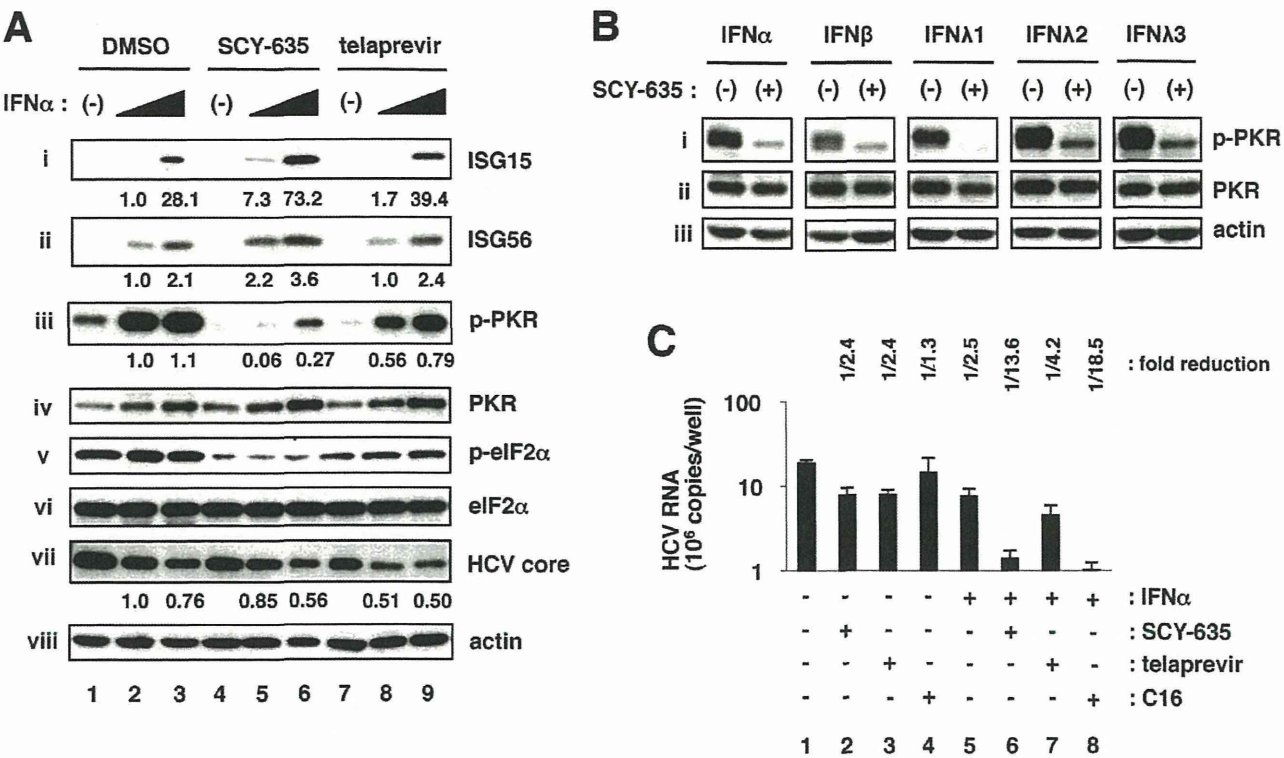

Figure 2. Phosphorylation of PKR was inhibited by SCY-635. (*A*) HCV-infected Huh-7 cells were treated with dimethyl sulfoxide (DMSO), 0.05%; SCY-635, 2 μM; or a protease inhibitor telaprevir, 2 μM for 24 hours, followed by treatment with or without IFNα (10 or 100 IU/mL) for 16 hours. Protein production of ISG15 (*i*), ISG56 (*ii*), phosphorylated PKR (T446) (*iii*), PKR (*iv*), phosphorylated eIF2α (S51) (*v*), eIF2α (*vi*), HCV core (*vii*), and actin (*viii*) are shown. Relative band intensities for these proteins by setting those in treatment with IFN alfa, 10 IU/mL plus DMSO as 1.0 are shown below the panels. (*B*) HCV-infected Huh-7 cells were pretreated with DMSO, 0.05% or SCY-635, 2 μM for 24 hours, and then treated with IFN alfa, 10 IU/mL; IFNβ, 10 IU/mL; IFNλ1 100 ng/mL; IFNλ2, 100ng/mL; or IFNλ3, 100 ng/mL for 16 hours. Proteins for phosphorylated PKR (T446) (*i*), PKR (*ii*), and actin (*iii*) were detected by Western blot. (*C*) SCY-635 as well as PKR inhibitor C16 enhanced the anti-HCV activity of IFN alfa. HCV-infected Huh-7 cells were treated with or without DMSO, 0.05% (*lanes 1* and *5*); SCY-635, 0.51 μM (*lanes 2* and *6*); telaprevir, 0.36 μM (*lanes 3* and *7*); or C16, 2 μM (*lanes 4* and *8*) together with (*lanes 5–8*) or without (*lanes 1–4*) IFN alfa, 10 IU/mL for 24 hours. HCV RNA in the cells was quantified by real-time reverse transcription polymerase chain reaction. Fold reduction values are also indicated above the graph.

levels of ISG proteins and phosphorylated PKR and eIF2α, in contrast, can be mediated by the elimination of HCV from the cells. SCY-635 also inhibited PKR phosphorylation triggered by another type-I IFN, IFN beta, and by the type-III IFNs, IFN lambda 1, IFN lambda 2, and IFN lambda 3 (Figure 2*Bi*). Previous reports have shown that highly phosphorylated PKR in HCV-infected cells reduced expression of ISG proteins on IFN-alfa treatment in an eIF2α-dependent manner.[29] These results suggest that SCY-635 restores ISG protein induction by preventing phosphorylation of PKR in HCV-infected cells.

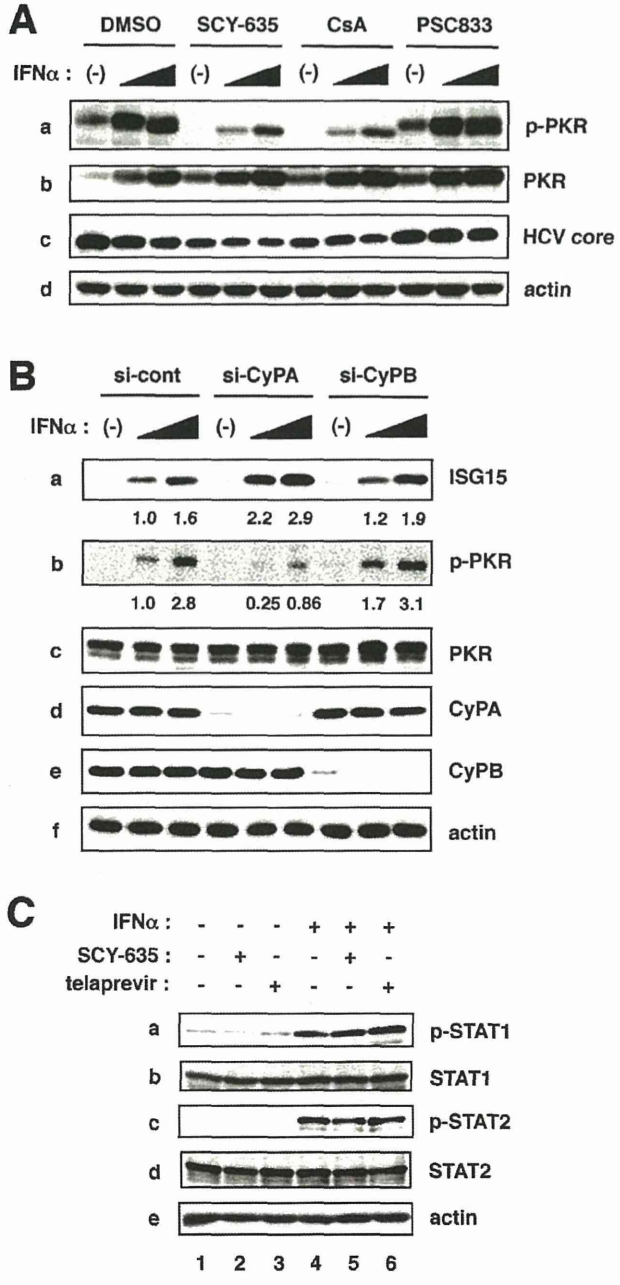

To examine whether the inhibition of PKR phosphorylation is really related to the anti-HCV activity, we treated HCV-infected cells with SCY-635 or telaprevir at the 50% effective concentrations, as well as C16, a PKR inhibitor, in combination with IFN alfa for 24 hours, and determined the HCV RNA level in these cells. Treatment with C16, while having only a slight anti-HCV activity on its own (Figure 2*C, lane 4*), drastically potentiated the anti-HCV activity of IFN alfa (Figure 2*C, lane 8*), supporting a suppressive role for phosphorylated PKR in IFN signaling as reported.[29] Importantly, treatment with SCY-635 together with IFN alfa dramatically reduced HCV RNA levels (Figure 2*C, lane 6*), although treatment with SCY-635 alone at this condition had only a limited anti-HCV effect (Figure 2*C, lane 2*). Cotreatment with telaprevir did not as notably augment the anti-HCV activity of IFN alfa (Figure 2*C, lane 7*), suggesting that the impairment of PKR phosphorylation contributed to the synergism for the anti-HCV effect of IFN-alfa treatment. Cotreatment with the identical concentrations of SCY-635 (2 μM) and IFN alfa (10 IU/mL) to those used in Figure 2*A* also showed a synergistic anti-HCV effect (Supplementary Figure 3*B*). Thus, PKR inhibition by SCY-635 can contribute to the elimination of HCV from infected cells in the presence of IFN alfa.

Cyclophilin A Played a Significant Role in Double-Strand RNA-Dependent Protein Kinase Phosphorylation and Interferon-Stimulated Gene Expression

To determine the factor responsible for the SCY-635-mediated impairment of PKR phosphorylation, we investigated the effect of 2 related compounds, CsA and PSC833. CsA is the prototype compound of SCY-635 and can inhibit CyP, while PSC833 is a CsA derivative deficient for CyP inhibition.[18] As shown in Figure 3*A*, pretreatment with SCY-635 or CsA, but not with PSC833, reduced the

Figure 3. CyPA was important for modulating PKR phosphorylation and ISG expression. (*A*) HCV-infected Huh-7 cells were treated with or without CsA or its derivatives, SCY-635 or PSC833. At 24 hours after treatment, cells were stimulated with IFN alfa at 10 or 100 IU/mL or left untreated for 16 hours. Proteins for phosphorylated PKR (T446) (*a*), PKR (*b*), HCV core (*c*), and actin (*d*) were detected by Western blot. (*B*) HCV-infected cells were transfected with small interfering (si) RNAs for CyP subtypes, CyPA (si-CyPA) or CyPB (si-CyPB), or with a nontargeting scrambled siRNA (si-cont). After 48 hours, cells were treated with or without IFN alfa at 10 or 100 IU/mL for 16 hours. Protein production of ISG15 (*a*), phosphorylated PKR (T446) (*b*), PKR (*c*), CyPA (*d*), CyPB (*e*), and actin (*f*) are shown. Relative band intensities are shown below the panels as in Figure 1*A*. (*C*) HCV-infected Huh-7 cells pretreated with dimethyl sulfoxide, 0.05% (*lanes 1* and *4*); SCY635, 2 μM (*lanes 2* and *5*); or telaprevir, 2 μM (*lanes 3* and *6*) for 48 hours were stimulated with (*lanes 4–6*) or without (*lanes 1–3*) 100 IU/mL of IFNα. Cell lysates were recovered at 60 minutes after treatment with IFN alfa. Proteins for phosphorylated STAT1 (Y701) (*a*), STAT1 (*b*), phosphorylated STAT2 (Y690) (*c*), STAT2 (*d*), and actin (*e*) were detected.

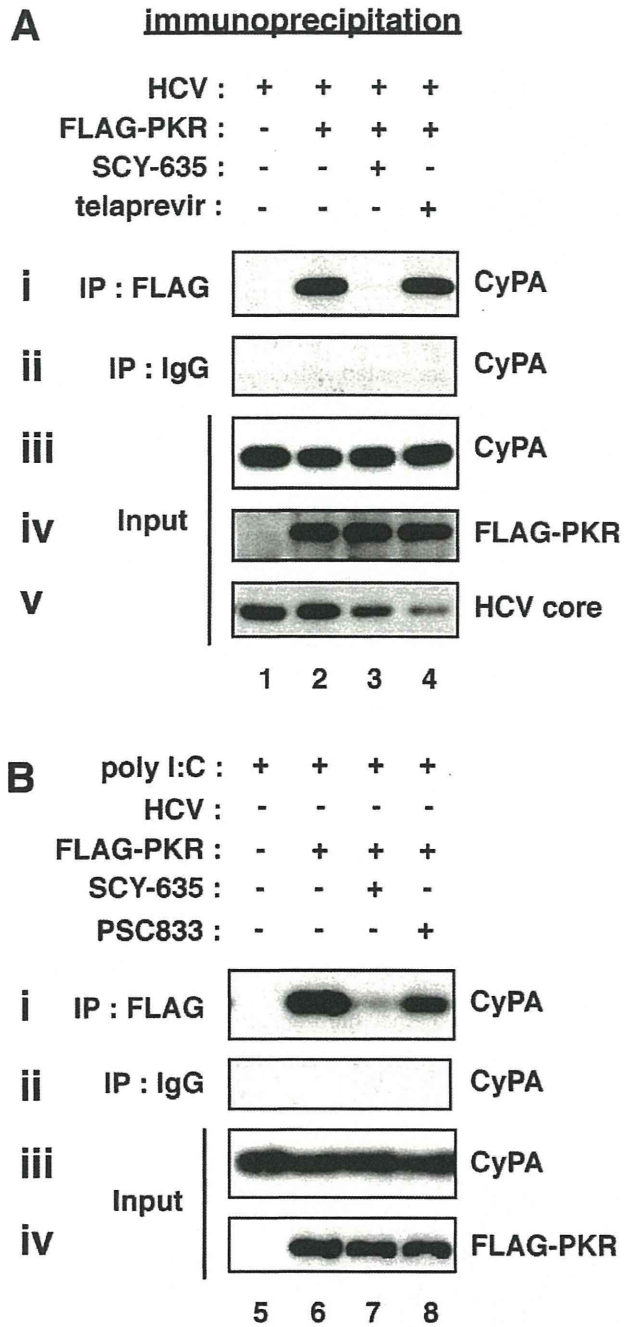

Figure 4. Interaction of PKR and CyPA in HCV-infected and poly I:C–stimulated cells. HCV-infected (*lanes 1–4*) and uninfected Huh7 cells (*lanes 5–8*) transfected with an expression plasmid for FLAG-tagged PKR (*lanes 2–4* and *6–8*) or the empty vector (*lanes 1* and *5*) for 6 hours were pretreated with dimethyl sulfoxide, 0.05%; SCY-635, 2 μM; telaprevir, 2 μM (*A*), or PSC833 2 μM (*B*) together with (*lanes 5–8*) or without (*lanes 1–4*) poly I:C for 24 hours. The cells were then stimulated with 100 IU/mL IFN alfa for 16 hours. Cell lysates were immunoprecipitated (IP) as described in Methods. Input, IP: FLAG, and IP: IgG indicate 10% input (*iii–v* in *A* and *iii–iv* in *B*), immunoprecipitation with an anti-FLAG antibody (*i*), and with a control anti-mouse normal IgG (*ii*), respectively. CyPA (*i–iii*), FLAG-PKR (*iv*), and HCV core (*v* in *A*) were detected by Western blot.

phosphorylation of PKR (Figure 3*Aa*), suggesting a critical role of CyP inhibition in the PKR dysregulation. Small interfering RNA-mediated knockdown of different CyP subtypes, CyPA and CyPB, indicated that a depletion of CyPB resulted in a slight increase in ISG15 production, as well as slightly increased phosphorylation of PKR (Figure 3*Ba*, and *b*), suggesting regulation of ISG15 production by a different mechanism independent of PKR. However, a knockdown of CyPA clearly augmented ISG protein production (Figure 3*Ba*), accompanied by a drastic reduction of PKR phosphorylation (Figure 3*Bb*). In general, CyPA is the most abundant protein among CyP subtypes and serves as the primary target of CyP inhibitors.[14] These data suggest that at least CyPA played a significant role in the regulation of PKR phosphorylation and the resultant ISG protein production.

SCY-635 Did Not Affect the Phosphorylation Status of Signal Transducers and Activators of Transcription 1 and 2

We investigated whether SCY-635 affected the phosphorylation status of other signaling components of the IFN pathway. Treatment with IFN alfa induced phosphorylation of STAT1 and STAT2 as shown in Figure 3*C* (*panels a* and *c, lane 4*). In this setting, pretreatment with SCY-635 or telaprevir did not have a significant effect on IFN alfa–induced phosphorylation of either STAT1 or STAT2 (Figure 3*C, panels a* and *c, lanes 5* and *6*). This is consistent with the result that SCY-635 did not change the transcription of ISG mRNAs (Figure 1*B*). Therefore, regulation of protein phosphorylation by CyPA was likely to be specific for PKR.

Cyclophilin A Interacted With Double-Strand RNA-Dependent Protein Kinase and Was Dissociated on SCY-635 Treatment

In general, CyPs regulate the function of their substrate proteins, such as IL2 tyrosine kinase, steroid hormone receptors, and adenine-nucleotide translocator, through direct molecular interaction.[35–37] We therefore investigated whether CyPA physically interacted with PKR in HCV-infected and uninfected cells. A co-immunoprecipitation assay from HCV-infected cells showed that endogenous CyPA co-precipitated with FLAG-tagged PKR (Figure 4*Ai, lane 2*). This interaction was dissociated by treatment with SCY-635, but not telaprevir (Figure 4*Ai, lanes 3 and 4*). To address whether the interaction between PKR and CyPA depends on the products derived from HCV, we conducted a co-immunoprecipitation assay in Huh-7 cells treated with poly I:C, which is generally used as a double-strand RNA mimic that can activate the IFN pathway, instead of with HCV. As shown in Figure 4*B*, endogenous CyPA co-precipitated with FLAG-tagged PKR in poly I:C–transfected cells, and this was abrogated by SCY-635 but not PSC833, a CsA derivative inactive for CyP inhibition (Figure 4*Bi, lanes 6–8*). In contrast, the interaction between CyPA and PKR was much less in the absence of HCV or poly I:C

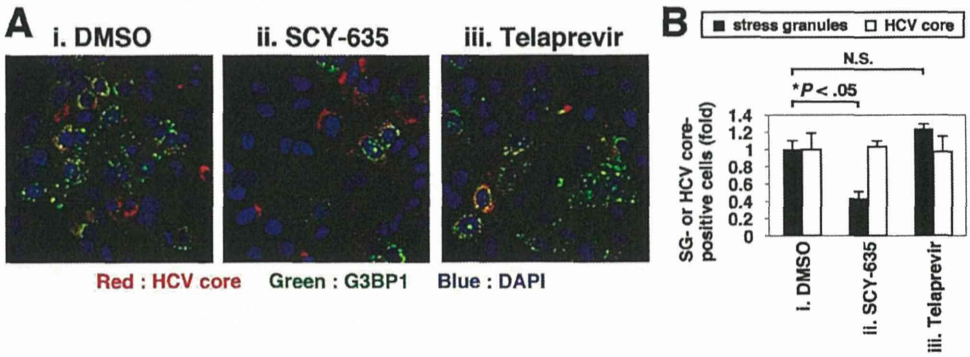

Figure 5. SCY-635 inhibited the formation of SGs. (*A*) HCV-infected Huh-7 cells were treated with dimethyl sulfoxide, 0.05% (*i*); SCY-635, 2 μM (*ii*); or telaprevir, 2 μM (*iii*) together with IFNα 100 IU/mL for 12 hours, and then were detected for G3BP1, an SG marker (*green*), HCV core protein (*red*), and the nucleus with 4′,6-diamidino-2-phenylindole (*blue*) by immunofluorescence analysis. The pictures show the merged pattern of 3 signals. (*B*) Numbers of SG-containing cells (*black bars*), as well as HCV core–positive cells (*gray bars*) were counted as Methods and are shown as relative values.

(Supplementary Figure 4). Therefore, the interaction of CyPA with PKR was likely to be more general to cells carrying double-strand RNA rather than specific for HCV-infected cells (also see Figure 6).

SCY-635 Inhibited Stress Granule Formation in Hepatitis C Virus–Infected Cells

Recent reports suggest that phosphorylated PKR plays a key role in the formation of SGs in HCV-infected cells.[31] The assembled SGs contribute to the suppression of IFN-alfa–triggered ISG translation.[30] We therefore examined whether SCY-635–mediated suppression of PKR phosphorylation and restoration of ISG translation were accompanied by an alteration of SG formation. Figure 5*A* shows the results of cells stained with G3BP1, a marker for SGs (*green*), as well as HCV core protein (*red*) and the nucleus (*blue*) in Huh-7 cells infected with HCV on IFN alfa treatment (Figure 5*A*). As shown in Figure 5*A* and *B*, treatment with SCY-635 decreased the number of cells forming SGs to approximately 40% of the control treated with IFN alfa and dimethyl sulfoxide (Figure 5*A* and *Bii*). In this condition in which the treatment time of anti-HCV agents was short, the number of HCV core-positive cells was not affected (Figure 5*A* and *Bii, iii*). In contrast, telaprevir did not decrease SG formation (Figure 5*A* and *Biii*), suggesting that the SCY-635 effect on SG formation was not the result of elimination of HCV from the cells, but rather through a direct effect on SG formation mediated by PKR.

Modulation of Double-Strand RNA-Dependent Protein Kinase by SCY-635 in the Absence of Hepatitis C Virus

To address whether the regulation of PKR by CyPA depends on products derived from HCV or not, we examined

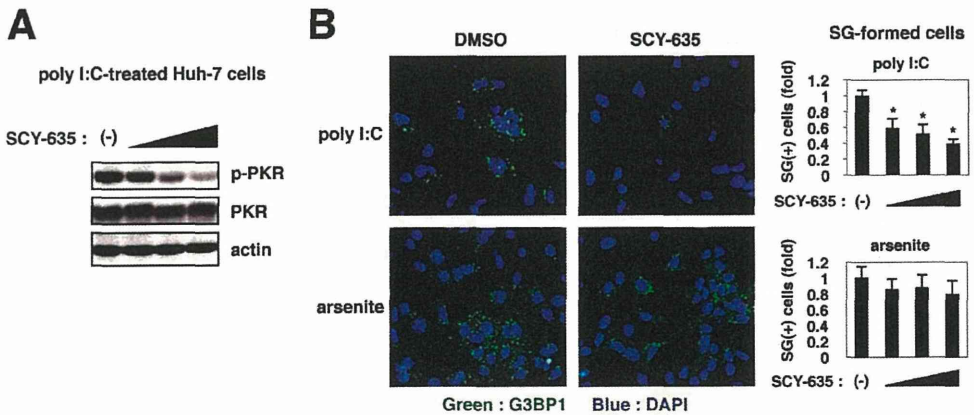

Figure 6. Modulation of PKR and SG formation by SCY-635 in the absence of HCV. (*A*) Huh-7.5.1 cells stimulated with poly I:C 0.5 μg/mL for 6 hours were pretreated with varying concentrations of SCY-635 (0, 2, 4, and 8 μM) for 18 hours. The cells were then treated with IFNα 100 IU/mL. At 24 hours later, phosphorylated PKR (T446), PKR, and actin were detected by Western blot (*A*). At 12 hours post treatment with IFN alfa, G3BP1 (*green*) and the nucleus (*blue*) were detected by immunofluorescence (*B, upper pictures*). For detecting PKR-independent SG, Huh-7.5.1 cells were pretreated with SCY-635 or dimethyl sulfoxide for 24 hours, followed by stimulation with arsenite 100 μM for 30 minutes to detect G3BP1 (*green*) and the nucleus (*blue*) (*B, lower pictures*).